AD-A067 701 ARMY ELECTRONICS RESEARCH AND DEVELOPMENT COMMAND WS--ETC F/G 4/1
RESPONSE CHARACTERISTICS OF KNOLLENBERG LIGHT-SCATTERING AEROSO--ETC(U)
FEB 79 R G PINNICK, H J AUVERMANN

UNCLASSIFIED ERADCOM/ASL-TR-0025 NL

1 OF 1
AD
A067701

END
DATE
FILMED
6-79
DDC

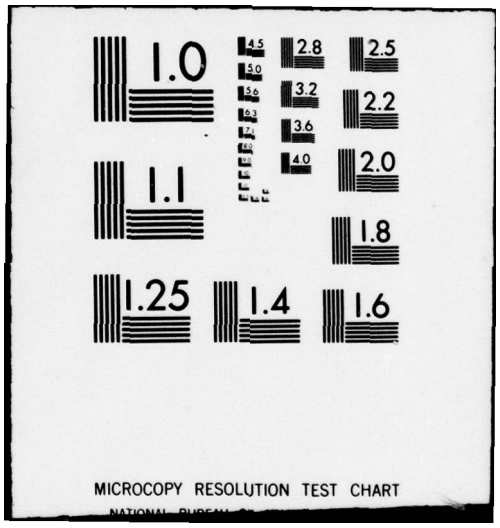
1.0
4.5
5.0
5.6
6.3
7.1
2.8
3.2
3.6
4.0
2.5
2.2
2.0
1.8
1.1
1.25
1.4
1.6
MICROCOPY RESOLUTION TEST CHART

ASL-TR-0025

AD

Reports Control Symbol
OSD - 1366

LEVEL II

12

AD A067701

RESPONSE CHARACTERISTICS OF KNOLLENBERG LIGHT-SCATTERING AEROSOL COUNTERS

FEBRUARY 1979

By

R. G. PINNICK
H. J. AUVERMANN

Approved for public release; distribution unlimited

US Army Electronics Research and Development Command
Atmospheric Sciences Laboratory
White Sands Missile Range, NM 88002

NOTICES

Disclaimers

The findings in this report are not to be construed as an official Department of the Army position, unless so designated by other authorized documents.

The citation of trade names and names of manufacturers in this report is not to be construed as official Government indorsement or approval of commercial products or services referenced herein.

Disposition

Destroy this report when it is no longer needed. Do not return it to the originator.

SECURITY CLASSIFICATION OF THIS PAGE (When Data Entered)

REPORT DOCUMENTATION PAGE

READ INSTRUCTIONS BEFORE COMPLETING FORM

(14) ERADCOM

1. REPORT NUMBER: ASL-TR-0025

2. GOVT ACCESSION NO.

3. RECIPIENT'S CATALOG NUMBER

4. TITLE (and Subtitle): (6) RESPONSE CHARACTERISTICS OF KNOLLENBERG LIGHT-SCATTERING AEROSOL COUNTERS.

5. TYPE OF REPORT & PERIOD COVERED: (9) R&D Technical Report

6. PERFORMING ORG. REPORT NUMBER

7. AUTHOR(s): (10) R. G. Pinnick, H. J. Auvermann

8. CONTRACT OR GRANT NUMBER(s)

9. PERFORMING ORGANIZATION NAME AND ADDRESS: Atmospheric Sciences Laboratory, White Sands Missile Range, NM 88002

10. PROGRAM ELEMENT, PROJECT, TASK AREA & WORK UNIT NUMBERS: (16) DA Task No. 1T161101A91A

11. CONTROLLING OFFICE NAME AND ADDRESS: US Army Electronics Research and Development Command, Adelphi, MD 20783

12. REPORT DATE: (11) Feb[redacted] 1979

13. NUMBER OF PAGES: 52

14. MONITORING AGENCY NAME & ADDRESS (if different from Controlling Office): (12) 56p.

15. SECURITY CLASS. (of this report): UNCLASSIFIED

15a. DECLASSIFICATION/DOWNGRADING SCHEDULE

16. DISTRIBUTION STATEMENT (of this Report): Approved for public release; distribution unlimited.

17. DISTRIBUTION STATEMENT (of the abstract entered in Block 20, if different from Report)

18. SUPPLEMENTARY NOTES

19. KEY WORDS (Continue on reverse side if necessary and identify by block number)

Light-scattering aerosol counters
In-situ measurement techniques
Knollenberg aerosol counters

79 04 18 015

20. ABSTRACT (Continue on reverse side if necessary and identify by block number)

Response calculations are presented for four commercially available "Knollenberg" light-scattering aerosol counters: the classical scattering aerosol spectrometer probe (CSASP), the active scattering aerosol spectrometer probe (ASASP), the forward scattering spectrometer probe (FSSP), and the axially scattering spectrometer probe (ASSP). These instruments are widely used in the Department of Defense for measurement of fog, haze, dust, smoke, and battlefield-debris aerosols, in many cases without adequate understanding of their response characteristics and limitations. The results presented here show sensitivity of the

next page

DD FORM 1 JAN 73 1473 EDITION OF 1 NOV 65 IS OBSOLETE

SECURITY CLASSIFICATION OF THIS PAGE (When Data Entered)

410 663

20. (ABSTRACT)

micrometer

response to aerosol refractive index for values of indexes characteristic of atmospheric aerosols, and for a particular index, multivalued response for particles in the 0.5μm to 4μm radius range. The response calculations have been validated for two of these instruments (the CSASP and ASASP) by measurement of monodisperse spherical particles. The size resolution of these two instruments is significantly less than advertised by the manufacturer and measurement of irregular particles causes additional loss of resolution.

PREFACE

The authors gratefully acknowledge the constructive review of this report by Glenn B. Hoidale and S. G. Jennings. In addition, we are indebted to Gerald W. Grams for use of his Mie computer programs, Ernest B. Stenmark for his programming assistance, and Robert McGrew for providing the scanning electron microscope micrographs that appear in this report.

CONTENTS

INTRODUCTION

Light-scattering aerosol counters are used for determination of size distribution and number concentration of aerosol particles. These devices work on the principle that as aerosol flows through an illuminated volume, light scattered by a single particle into a particular solid angle is measured and used to determine particle size by electronically classifying response pulses according to their magnitude. Determination of particle size from the response is indirect because of the dependence of the response on factors other than particle size, namely, particle shape and complex index of refraction; lens geometry of the counter optical system; and for broadband sources, phototube spectral sensitivity. A number of theoretical and experimental studies of response characteristics of light scattering counters have been done for several commercially available instruments [1-5] and those of special design [6-14]. In the research discussed in this report, the response characteristics of four models of "Knollenberg" (after R. G. Knollenberg, the developer) light scattering counters that have recently become commercially available (Particle Measurement Systems [PMS], Boulder, Colorado) were investigated. These instruments are widely used for aerosol measurement, perhaps indiscriminately and without adequate understanding of their response characteristics and limitations. An understanding of these factors is needed to assess errors in measurements made with them. In this report an attempt is made to gain this understanding.

Measurements of known monodisperse aerosols are highly desirable for investigating counter response. Thus, the next section gives a brief account of techniques used for generation of both spherical and irregular monodisperse aerosols. The third section presents a general description of the optical systems of the four Knollenberg counters: the classical scattering aerosol spectrometer probe (CSASP), the active scattering aerosol spectrometer probe (ASASP), the forward scattering spectrometer probe (FSSP), and the axially scattering spectrometer probe (ASSP). The fourth section presents the theoretical methods used for calculation of these counters' response for spherical particles, and the fifth section presents a comparison of theoretical and experimental results for the CSASP and ASASP using both monodisperse spherical and irregular particles. Finally, theoretical response calculations of all the instruments are presented for spherical particles with refractive indexes representative of atmospheric aerosol constituents.

GENERATION OF MONODISPERSE AEROSOLS

To definitively measure the response characteristics of aerosol counters, one must be able to generate aerosols of uniform size and different composition (or refractive index). For these studies uniform particles of nigrosin dye, sodium chloride, and potassium chlorate were generated by the vibrating orifice technique described earlier [6]. In this technique, the aerosol material is dissolved in a volatile solvent (water) and the resulting solution is forced at high pressure through a small (5μm to 20μm diameter) orifice. A transducer is attached to the

orifice, and at certain resonant frequencies the jet of solution squirting through the orifice breaks under the action of surface tension into droplets of uniform size. The volatile components of the droplets evaporate, leaving the residual aerosol.

The size of the aerosol depends on the concentration of material in solution, orifice size, orifice pressure, viscosity of the solvent used, and resonant frequency. For example, one part per thousand nigrosin dissolved in water forced through a 10μm orifice at 20 psi results in a resonance at 163 kHz and generation of aerosol of 2.12μm radius following evaporation of the solvent. An aerosol particle is generated for each complete vibration of the orifice. The standard deviation in particle size of aerosol made with this technique is on the order of 2 percent of the mean diameter, not counting particles that coalesce before drying, forming particles two, three, and four times larger in volume. This aerosol generation technique is essentially the same as that of Bergland and Liu [15]. In fact, a modified Bergland and Liu generator (commercially available from Thermal Systems, Inc., Minneapolis, MN) was used. The modification consisted of replacing the syringe pump with a compressed air source held at constant pressure.

Monodisperse spherical aerosols of polystyrene, polyvinyltoluene, and styrene divinylbenzene latexes available from Dow Chemical in the hydrosol were generated by nebulizing hydrosol samples diluted with distilled water. Also, nearly monodisperse crown glass beads available from Particle Information Services were generated by simply shaking the beads from their vial container. A summary of monodisperse aerosols utilized in this study is shown in table 1.

THE PARTICLE COUNTERS

Figure 1 shows a schematic of the CSASP optical system modified from a drawing supplied by the manufacturer. The instrument is essentially a dark-field microscope with silicon photodiodes used as the detectors. Air containing aerosol being sampled is drawn through the focal point of the collecting optics where individual particles scatter light into the microscope and photodetectors. The source of illumination is a 5 mW He-Ne laser tuned to a high order random mode. The optical system has axial symmetry with respect to the direction of the laser source and permits collection of light scattered 4 to 22 degrees from the direction of forward scattering.

The output of the photodetector is a measure of the intensity of light scattered by single particles and is fed into a 15-channel pulse-height analyzer. Figure 2 shows a typical CSASP spectrum for monodisperse aerosol of nigrosin dye together with a scanning electron microscope micrograph of several of these particles collected onto a Nuclepore filter. The peak in channel 12 corresponds to the most frequently occurring scattered intensity for this aerosol and its position is proportional to the counter response. The spread in the peak is caused by statistical broadening, nonuniform illumination of the sample volume,

and variation in aerosol size. For irregular particles a broader spectrum of pulse heights is measured, as different particle orientations result in distinctly different response pulses, even for particles nearly identical in shape. The spectrum in figure 3 shows this effect for uniform slightly irregular particles of sodium chloride; the figure also shows a micrograph of typical salt particles corresponding to this spectrum. This spectrum would be more nearly Gaussian if pulse height were plotted on the abscissa rather than channel number, as the channels are not of equal width. The size resolution of the instrument is obviously degraded for irregular particles.

The light-collecting optics of the ASASP instrument are identical to those of the CSASP, but in this case the particle illumination source is the intracavity standing wave radiation of a hybrid 2 mW He-Ne laser [16]. An advantage of utilizing the open-cavity source is the high energy density available (about 1 kW/cm^2 according to PMS), permitting measurement of particles down to about 0.1μm radius. Pulse height spectra for monodisperse spherical and irregular particles for this instrument are similar to those for the CSASP.

Only a small fraction of the particles which pass through the relatively large intakes of the CSASP and ASASP instruments, which consist of a conical horn with minimum diameter 3.3 cm, is counted. The relatively small volume through which particles must pass before they are counted is determined opto-electronically. Signals which derive from particles that do not flow through a particular volume which is within a sufficiently uniformly illuminated part of the laser beam are out-of-focus and electronically rejected.

Both FSSP and ASSP instruments are similar to the CSASP in that they are forward-scattering instruments and the illumination source is a He-Ne laser. The optical systems permit collection of light scattered 3 to 13 degrees (for the FSSP) and 5.3 to 12.4 degrees (for the ASSP) from the direction of forward scattering. In both instruments the coincidence scheme for particle detection involves a time-of-flight measurement of single particles traversing the laser beam and subsequent rejection of particles passing through the beam edges.

Table 2 summarizes the characteristics of the light-scattering counters.

THEORETICAL RESPONSE CALCULATIONS

In this section the theoretical methods used for calculating particle counter response are outlined by using Mie theory for the CSASP, FSSP, and ASSP instruments and a solution for scattering of standing wave radiation by a spherical particle for the ASASP.

From Mie theory for a polarized plane wave having wavenumber k incident on a sphere with radius r, the scattering cross section (in cm^2 per

particle) for radiation scattered into a solid angle having axial symmetry with respect to the direction of the light source is:

$$R = \frac{\pi}{k^2} \int_{\Omega} \left\{ \left|S_1\right|^2 + \left|S_2\right|^2 \right\} \sin\theta \, d\theta \tag{1}$$

where $S_1(x,m,\theta)$ and $S_2(x,m,\theta)$ are the Mie scattering amplitude functions corresponding to light polarized with electric vector perpendicular and parallel to the plane of scattering. They depend on the particle size parameter $x = kr$, the refractive index m, and the scattering angle θ. The angular integration is over the solid angle Ω subtended by the light-collecting optics.

Because the scattering for the ASASP is for a particle in a standing wave, the scattering amplitude S' is calculated by adding the Mie scattering amplitudes for plane waves traveling in opposite directions: $S'(\theta) = S(\theta) + S(\pi - \theta)$. The response for the ASASP is then

$$R = \frac{\pi}{k^2} \int_{\Omega} \left\{ \left|S_1(\theta) + S_1(\pi - \theta)\right|^2 + \left|S_2(\theta) + S_2(\pi - \theta)\right|^2 \right\} \sin\theta \, d\theta \tag{2}$$

RESULTS

Measurements of the CSASP and ASASP response to monodisperse spherical latex and nigrosin dye aerosols are presented in figures 4 and 5 as open and solid circles. The radii of the latex particles are those advertised by Dow Chemical; those for nigrosin were measured by scanning electron microscope. The error in radius is not more than the width of the circles marking the measurements.

The measured response is expressed in cross section per particle normalized to the computer calculated theoretical results (solid-line curves) for best fit to the theoretical response for latex aerosols. This single normalization was used for all experimental results for each instrument. Polystyrene, polyvinyltoluene and styrene divinylbenzene latex aerosols actually have three similar but distinct indexes of refraction (see table 1); however, the response curves for these indexes are not significantly different and therefore only the response curve for polystyrene latex with index 1.592-0i is shown. Error in measurement of response is due to the finite width of the instrument pulse height channels and instrument drift. Repeated measurement of polystyrene latex particles showed instrument drift to be ± 10 percent in pulse height over a period of 1 month.

Also shown in figure 4 is the CSASP response to relatively narrow polydispersions of glass beads having refractive index 1.51-0i. The measured response is denoted by the squares and the theoretical response by the dashed curve. The standard deviation in particle size of the beads is indicated by the horizontal "error" bars and at least 68 per-

cent of the signals for these particles have pulse heights falling between the vertical "error" bars.

Figure 4 indicates that the theoretical response for the CSASP is corroborated by measurements on uniform aerosols with three markedly different indexes of refraction and with radii 0.30μm to 10μm. Therefore the Mie theory calculated response according to equation (1) adequately predicts the CSASP response for spheres, regardless of effects that may be caused, as suggested by the manufacturer, by multimode operation of the instrument laser source. The theoretical results according to equation (2) for the ASASP instrument are also verified by the response measurements in figure 5, with the exception of particles with radii greater than about 1μm. The extinction cross section of these larger particles is apparently sufficient to cause appreciable reduction in laser power and consequent deviation from the theoretical response curve.

The CSASP and ASASP response to slightly irregular randomly oriented uniform particles of sodium chloride and potassium chlorate have also been measured. These results, shown compared to theoretical response calculations again according to equations (1) and (2) for spheres of equivalent cross-sectional area, are shown in figures 6 through 9. As before, the experimental results are normalized to the measured response for polystyrene so that the comparison of experiment and theory here is absolute. Measurements of uniform irregular particles with these instruments result in a range of pulse heights and hence broader spectra than for spheres, as can be seen by comparing spectra in figures 2 and 3. Here the response plotted corresponds to the most frequent scattered intensity for the randomly oriented particles and at least 68 percent of the monodisperse aerosol counted have pulse heights falling between the vertical "error bars."

Figures 10 and 11 show micrographs of typical monodisperse particles of sodium chloride and potassium chlorate collected onto Nuclepore filters. Although it may not be obvious from these telescoping micrographs, sodium chloride particles with equivalent radius less than 3μm (as in figure 10, lower micrographs) consist of assemblies of cubes with a hollow center; larger particles (as in figure 10, upper micrographs) have five flat sides and one rounded side with a hole in the center. Potassium chlorate particles are prolate ellipsoids with rough surfaces and also some irregularly shaped voids within.

Thus, comparison of measurements in figures 6 and 7 (for the CSASP) and figures 8 and 9 (for the ASASP) shows comparable response for particles of markedly different shape (sodium chloride and potassium chlorate).

Potassium chlorate is birefringent; however, no theory exists for calculating scattering for birefringent particles. Consequently in figures 7 and 9 the measured response for potassium chlorate is compared to two theoretical curves: one curve for homogeneous spherical particles having index of refraction of the ordinary ray ($m = 1.52-0i$), and one

for particles having index of refraction of the extraordinary ray ($m = 1.409-0i$). These two response curves are only significantly different in the 0.5μm to 2μm radius range. It is noteworthy that both of the theoretical curves are in poor agreement with the measurements for particles in this size range, although for smaller and larger sizes, where the two theoretical curves are similar, the measurements are in better agreement with the theoretical response curves.

For the CSASP both the sodium chloride and potassium chlorate results show: (1) rough agreement of measurement and theory for equivalent radii $1.5\mu m < r < 4\mu m$, (2) the resonance behavior in the calculated response is not evident in the measured response, (3) slightly smaller response measured than predicted for particles with equivalent radius $\gtrsim 4\mu m$, and (4) a resonance in the measured response for particles with equivalent radius 0.8μm which may be a consequence of the shell-like structure of the particles.

The following geometrical optics argument is offered to explain the general agreement of the measured response for irregular particles and that predicted for spheres of equal cross-sectional area, providing equivalent radii are between 1.5μm and about 4μm. First, particles must have equivalent radii $r \gtrsim 1.5\mu m$ (or size parameters $x \gtrsim 15$) for geometric optics to apply. Thus, if particles have $r \gtrsim 1.5\mu m$, and if light scattered within the forward lobe is sensed, diffraction is dominant; and to the first order only the projected area of the particle is important. Thus, low-angle scattering constitutes a somewhat reliable measure of particle projected area for particles of irregular shape, providing they are sufficiently large ($r \gtrsim 1.5\mu m$). On the other hand, they cannot be too large, since if light scattered primarily outside the forward lobe is sensed, as it is for particles with equivalent radius $r \gtrsim 4\mu m$, reflection and refraction contributions are liable to produce a response which deviates considerably from that of a sphere of equal area, as the measurements show in figures 6 and 7. These measurements suggest that the CSASP response to even larger ($\gtrsim 6\mu m$ equivalent radius) irregular particles might result in significant underestimation of particle sizes. Response measurements for more irregular and larger particles is an obvious deficiency of this work.

For the ASASP the irregular particle measurements show agreement of measured and theoretical response for particles with equivalent radius $r \lesssim 0.5\mu m$ but disagreement for larger sizes and virtually no size resolution for particles with $r \gtrsim 0.5\mu m$.

For the special case of spherical particles, the measurements corroborate the theoretical response curves for both the CSASP and ASASP, with the exception of particles having radius $\gtrsim 1\mu m$ for the ASASP, which apparently cause significant reduction in laser power. Confidence can thus be placed in response calculations for materials with refractive indexes

different from those studied here. Response calculations for refractive indexes typical of atmospheric constituents at $\lambda = 6328\text{Å}$ ranging from the refractive index of water ($m = 1.33-0i$) to carbon ($m = 1.95-0.66i$) were consequently carried out and are presented in figures 12 (CSASP) and 13 (ASASP). The pulse height discriminator levels, as set by the manufacturer for our particular models of these instruments, are shown by the tick marks in these figures. There are 15 particle size channels for each "range" of the instruments; channels 1, 5, 10, and 15 are labeled between the appropriate tick marks. Changing range is merely an adjustment of amplifier gain for the CSASP (for the ASASP both amplifier gain and discriminator level settings are different for each range) and has the effect of shifting the size range of sensitivity.

Users of these counters are warned that discriminator levels for different CSASP and ASASP instruments are not necessarily set as shown in figures 12 and 13, as the manufacturer has a number of different schemes for setting these levels. Nevertheless, the manufacturer utilizes several sizes of polystyrene, polyvinyltoluene and styrene divinylbenzene latex particles and glass beads in the factory "calibration," identified according to what channel they are counted as per the instrument manual supplied with each instrument. This information enables the user to infer positions of discriminator level settings relative to the theoretical results presented here.

Comparison of the CSASP and ASASP theoretical response curves for both absorbing and nonabsorbing aerosols show they are quite similar, the ASASP having high frequency wiggles in its response for particles in the resonance region (i.e., in the region where particles have sizes comparable to the wavelength), which are not found in the CSASP response. This result for a particular refractive index can be seen in figure 14, where the CSASP and ASASP response to particles with $m = 1.54-0i$ are compared.

It is hardly necessary, in light of these results, to stress the fact that for spherical particles both the CSASP and ASASP responses are sensitive to aerosol refractive index over the range of realistic values for these indexes. For example, for the CSASP (figure 12), water particles ($m = 1.33-0i$) with radii 5μm have identical response to dust particles ($m = 1.50-0.005i$) with radii 10μm. Even for aerosol of known composition there are, on some ranges of the instruments, discriminator levels set in regions of multivalued response. Thus for the CSASP, water particles with radii 0.63μm, 0.94μm, and 1.3μm all have the same response. Nevertheless, size distribution information for a polydispersion of homogeneous particles can be determined by reducing the number of channels to avoid these regions.

For example, if the CSASP is used to measure fog droplets, the channels can be grouped according to the response curve for water to avoid regions of multivalued response. This channel grouping is indicated by the heavy tick marks in figure 12. The channels are grouped with less size resolution than the response curve dictates because, in practice,

statistical spectra broadening effects result in some channel cross sensitivity. As was pointed out previously, even measurements of monodisperse spherical aerosol result in a range of pulse heights, and identical particles are not counted entirely in one particle size channel. Therefore, use of discriminator levels set near regions of multivalued response has been avoided. This scheme reduces the number of size channels for each range from 15 to 8. Specific channel size limits for the different ranges of the instrument can be determined for figure 12 by noting at what radii on the water response curve the appropriate heavy tick marks correspond.

A comparison of channel size limits determined in this way compared to limits advertised by the manufacturer is given in table 3. Not only is the size resolution of the CSASP generally reduced, but the channel limits differ by as much as a factor of two from the advertised values. Measurements of spherical particles having refractive indexes different from water would of course require different channel groupings and size definitions.

If the manufacturer's calibration is used in determination of size distribution of polydispersions of spherical particles, artificial knees or bumps in the distribution will appear in regions of multivalued response. These knees or bumps appear because in these regions particles with a relatively large range of sizes produce response pulses in a small range of pulse heights; whereas, between regions of multivalued response, particles with a relatively narrow range of sizes produce response pulses in a comparable range of pulse heights. The resulting artifacts have been seen in the manufacturer calibration-derived distribution for the CSASP both in measurements of atmospheric fog and in measurements of laboratory generated polydispersions of oil droplets. The positions of these knees in the distributions are of course different for particles with different refractive indexes. Recently reported measurements of atmospheric aerosols by Livingston [17] with the Knollenberg ASASP show knees in the distribution in the region of multivalued response for water droplets (as per figure 13) which we suggest are simply artifacts of the instrument response, and not real.

The FSSP and ASSP light scattering counters are similar to the CSASP; the essential difference being geometry of their light-collecting optics (see table 2). Theoretical response calculations for these instruments, again according to equation (1), are presented in figures 15 and 16. Like the CSASP, the response is sensitive to particle refractive index over a range of indexes characteristic of atmospheric aerosols; the ASSP has particularly poor resolution in the 1μm to 4μm radius range. The positions of the factory-adjusted discriminator level settings relative to the theoretical results presented here can be determined by noting in what channel sodalime glass beads or polystyrene spheres of a particular size are counted. This information is given in the manual supplied with each instrument. The position of the channel in question can then be determined from the theoretical response curves. In the case of glass beads, the response curves for refractive index m = 1.50-0i in figures

15 and 16 can be used (although the refractive index of the glass beads is m = 1.51-0i, the response curve for m = 1.51-0i is well approximated by that for m = 1.50-0i). In the case of polystyrene or polyvinyltoluene latex spheres, the response curves for m = 1.592-0i given in figure 17 may be used.

Both the FSSP and ASSP instruments utilize near-forward scattering and as argued previously should offer a somewhat reliable measure of particle cross section for irregular particles less than a certain size. Otherwise, measurement of their response to known irregular particles is needed.

A terse summary of findings for the four Knollenberg light scattering counters is given in table 4. For the CSASP and ASASP instruments, the manufacturer generally specifies more particle size channels than can be justified, particularly for particles with radii greater than 0.5μm. The theoretical results suggest the same is true for the FSSP and ASSP, although the authors do not have information on the discriminator level settings for these instruments.

Finally, although the question of the counting efficiency of these light scattering counters is not addressed in this report, the authors are aware of two potential problems with the CSASP instrument that might be important for the other instruments too. The first problem concerns the coincidence scheme utilized in the CSASP to reject or accept particles depending on whether or not they pass through the relatively small "sample volume." Only a small fraction ($\sim$0.003 percent) of particles flowing through the instrument are actually measured. The purpose of the coincidence scheme is to reject particles which are not within a sufficiently uniform part of the laser beam by opto-electronically discriminating against out-of-focus particles. According to the manufacturer there are on the order of ten particles rejected for every one counted. There is evidence to suggest that this scheme results in a sample volume that is somewhat dependent on particle size. In other words, the instrument flow rate may be different for different size channels. However, simultaneous measurements made on uniform aerosols in our laboratory with both the CSASP and a particle counter of a special design developed by Rosen [18] show agreement in absolute aerosol concentration to within 30 percent for particles with radii of about 1μm. Some preliminary results on the ASASP indicate much larger errors for submicron particles.

The second potential problem concerns errors due to nonisokinetic sampling. Air containing aerosol sampled under a no-wind condition with the particular aspirated CSASP the researchers used flows at 340 liters per minute through a conical intake tube 45 cm long with maximum diameter 10 cm and minimum diameter 3.3 cm. The fraction of particles lost in this tube due to gravitational settling depends strongly on size and is estimated 7 percent for 15μm radius particles, increasing to 18 percent for 25μm radius particles, under the assumption particle density is

1 gcm^{-3}. The magnitude of errors due to nonisokinetic sampling during windy conditions is unknown.

CONCLUSIONS

Theoretical response calculations for two models of Knollenberg light scattering aerosol counters (the CSASP and ASASP) have been compared to measurements of monodisperse aerosols of different size and refractive index. The theoretical predictions for the CSASP, which are based on Mie theory, are verified by the measurements on spherical particles with radii 0.3μm to 10μm. The ASASP predictions are derived from a solution for scattering by a sphere in a standing wave and are also validated by measurements on spherical particles with radii 0.12μm to 1μm. Particles larger than 1μm radius, which is near the upper limit of detectability for the ASASP, apparently have sufficiently large extinction cross section to cause significant reduction in laser power and disagreement of predicted and measured response results. In any case both instruments show sensitivity of response to aerosol refractive index over the range of values of indexes realistic for atmospheric aerosol. This sensitivity results in poorer size resolution than advertised for these counters, as two aerosol particles differing in size by as much as a factor of three may be counted in the same size channel. For aerosol of known composition, size resolution is much improved, although not as good as advertised since size channels must be grouped to avoid regions of multivalued response. As might be expected, measurement of irregular particles causes further degradation in resolution, because of the importance of particle orientation.

For the Knollenberg FSSP and ASSP light scattering counters, the theoretical predictions of response for spheres again show sensitivity to aerosol refractive index and the attending loss of size resolution.

Generally, the best size resolution is obtained with these instruments for measurement of homogeneous spherical aerosols such as fog and some military smokes (such as FS, RP, fog oil, nitric acid, diesel oil, and silicone oil). However, measurement of battlefield-debris aerosol, which might contain irregular dust and high explosive debris particles of mixed composition, would result in relatively poor size resolution.

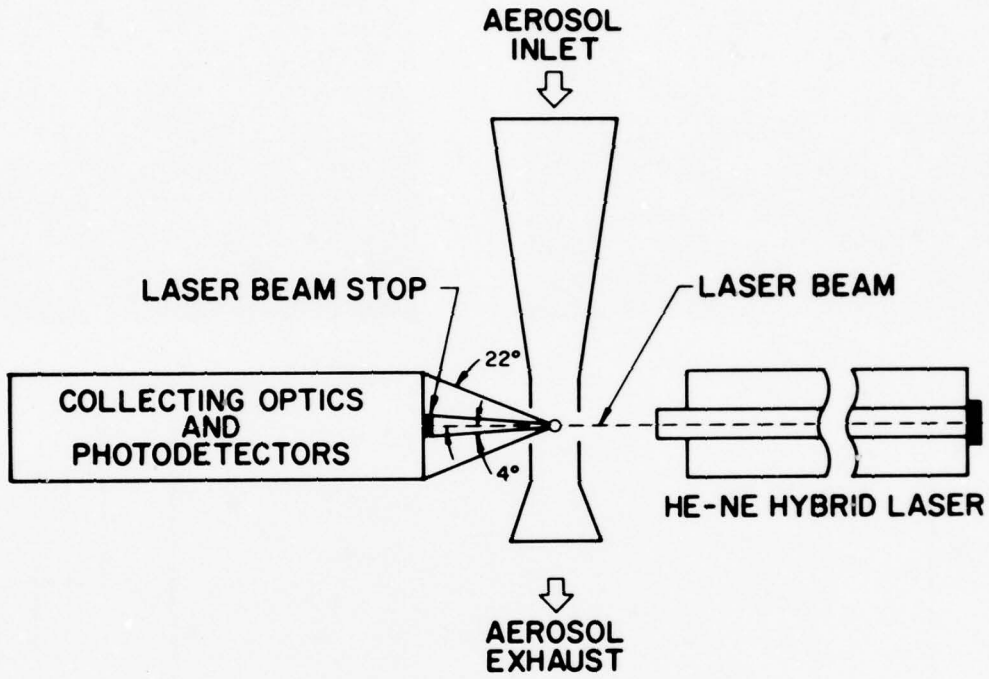

Figure 1. Schematic of the Knollenberg CSASP light scattering aerosol counter

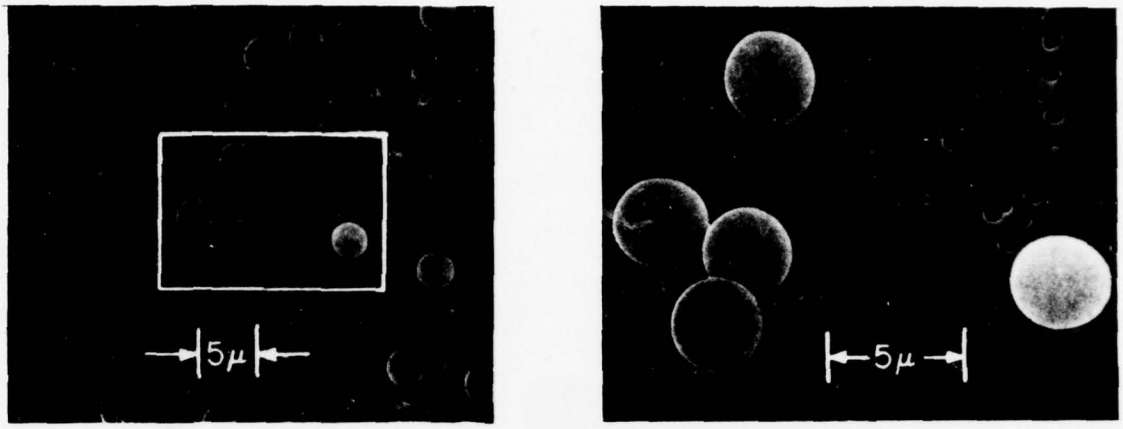

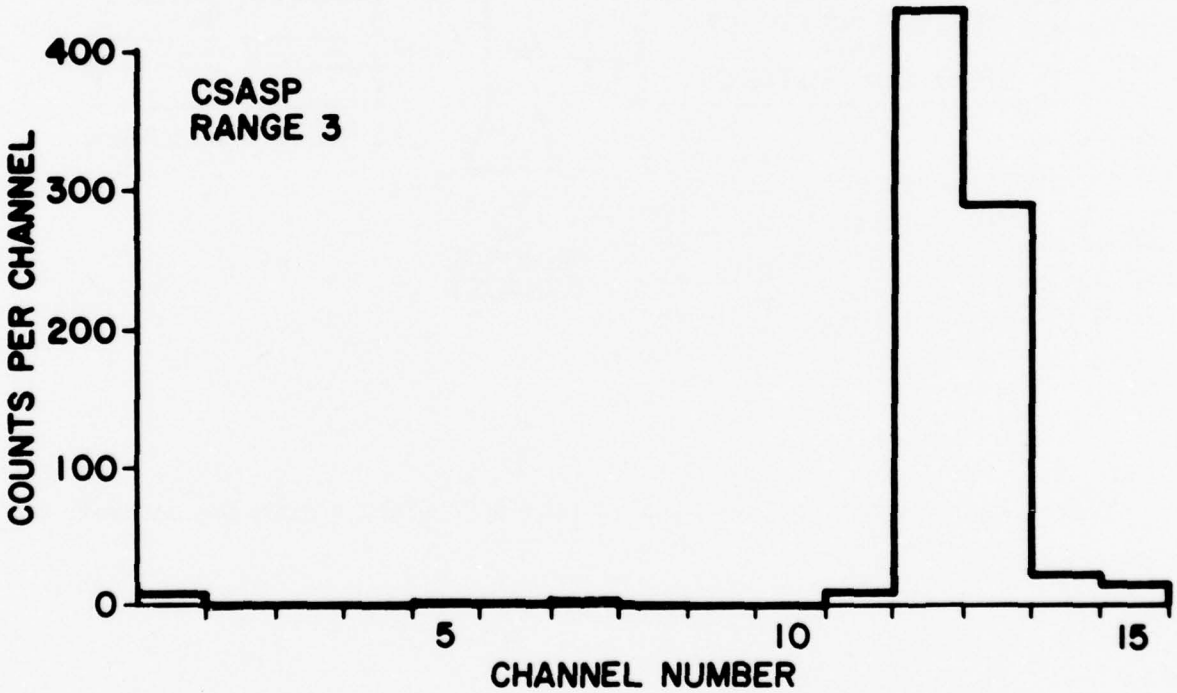

Figure 2. A typical CSASP pulse height spectrum for monodisperse aerosol. This particular spectrum is for solid particles of nigrosin dye with mean radius 1.78μm; a scanning electron microscope micrograph of several of these particles collected onto a Nuclepore filter is also shown.

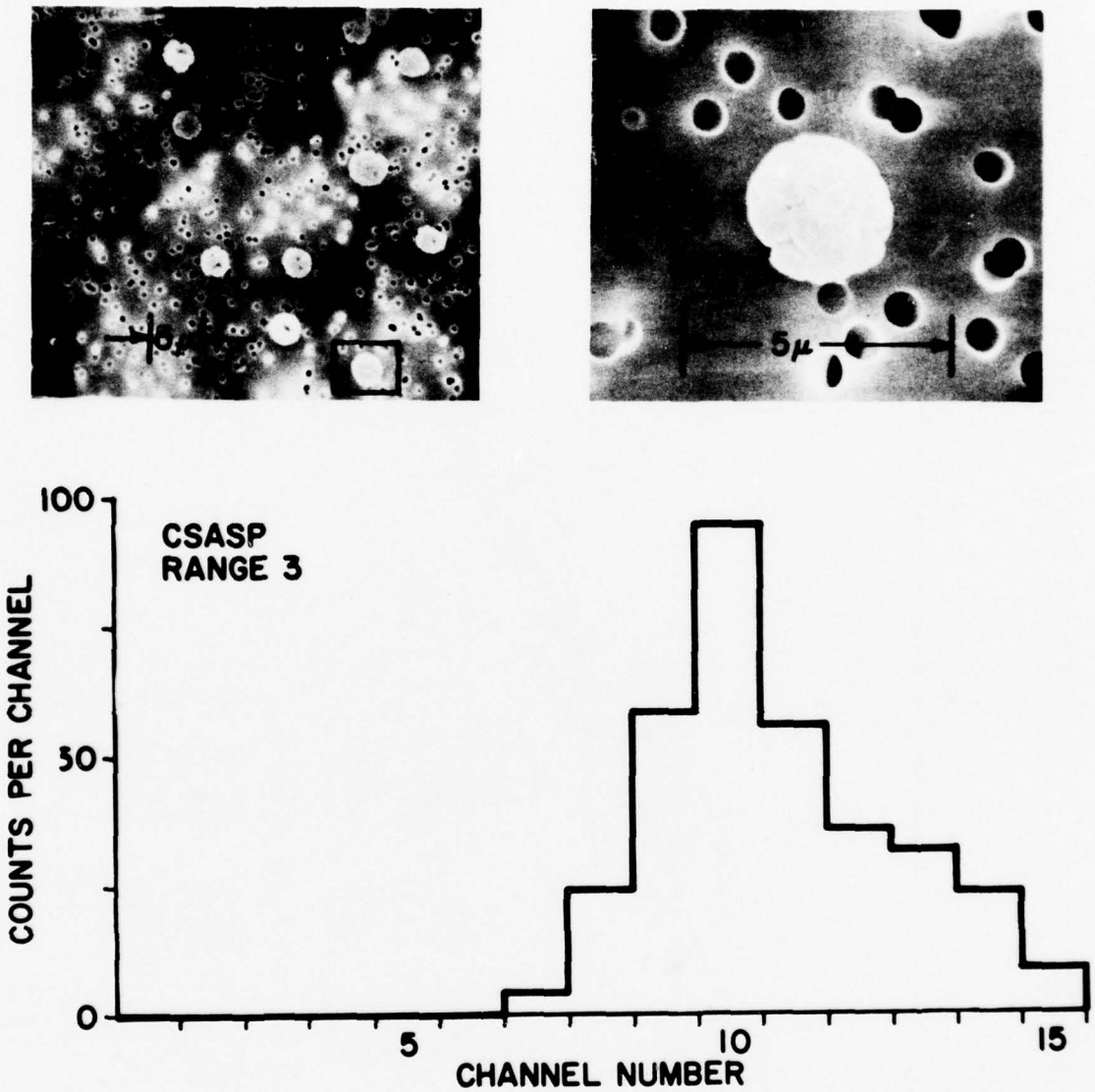

Figure 3. A typical CSASP pulse height spectrum for monodisperse aerosol particles that are irregular in shape. This spectrum is for sodium chloride particles with mean equivalent radius 1.53μm (in the sense of spheres of equal cross-sectional area); a micrograph of several of these particles collected onto a Nuclepore filter is also shown.

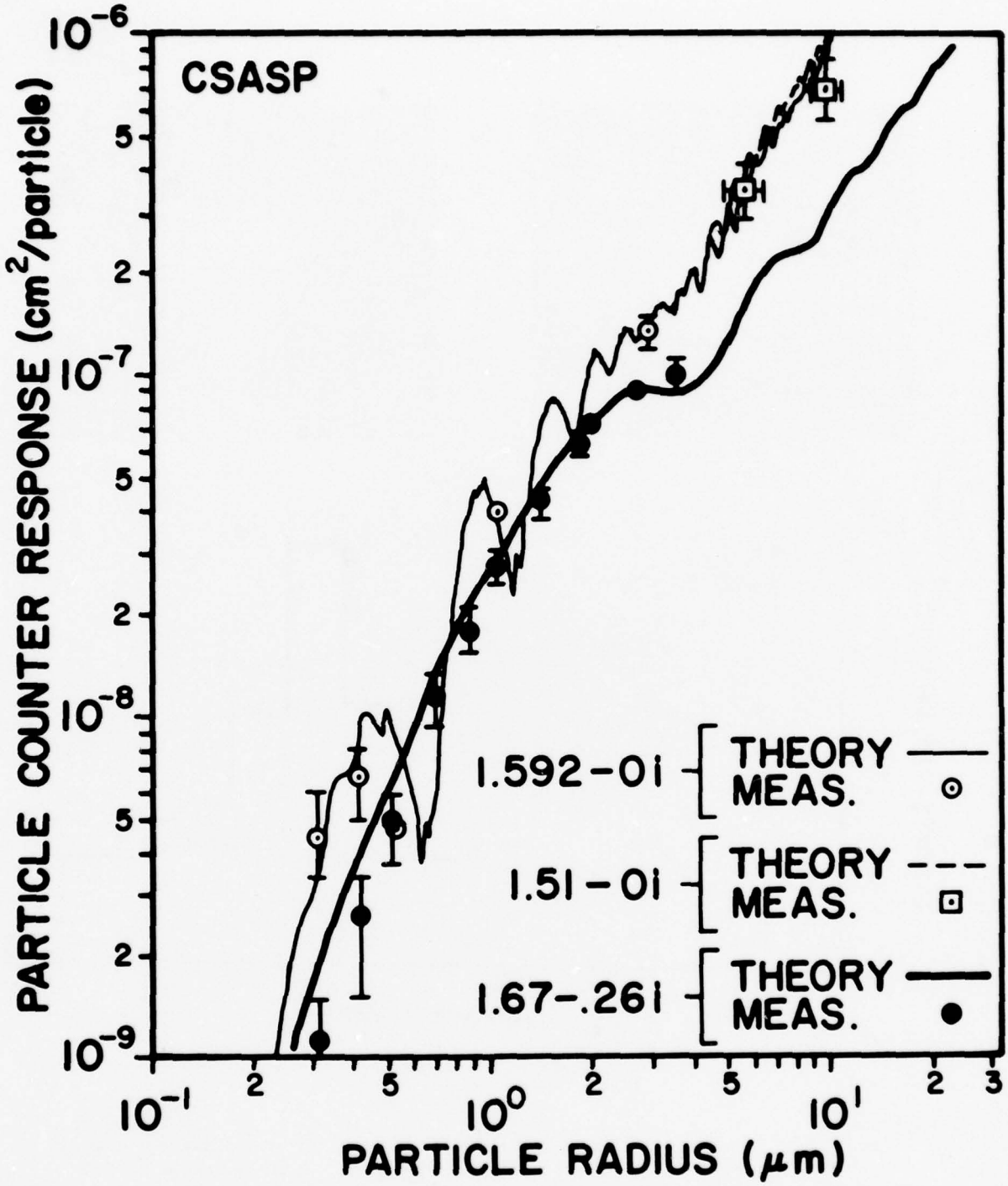

Figure 4. Knollenberg CSASP response: measured (circles and squares) and calculated using Mie scattering theory (curves) for single spherical particles versus particle size. The measurements have been normalized for best fit to the calculated response for polystyrene latex particles with refractive index m = 1.592-0i. The theoretical curve for glass beads with refractive index 1.51-0i extends down only to about 5μm radius.

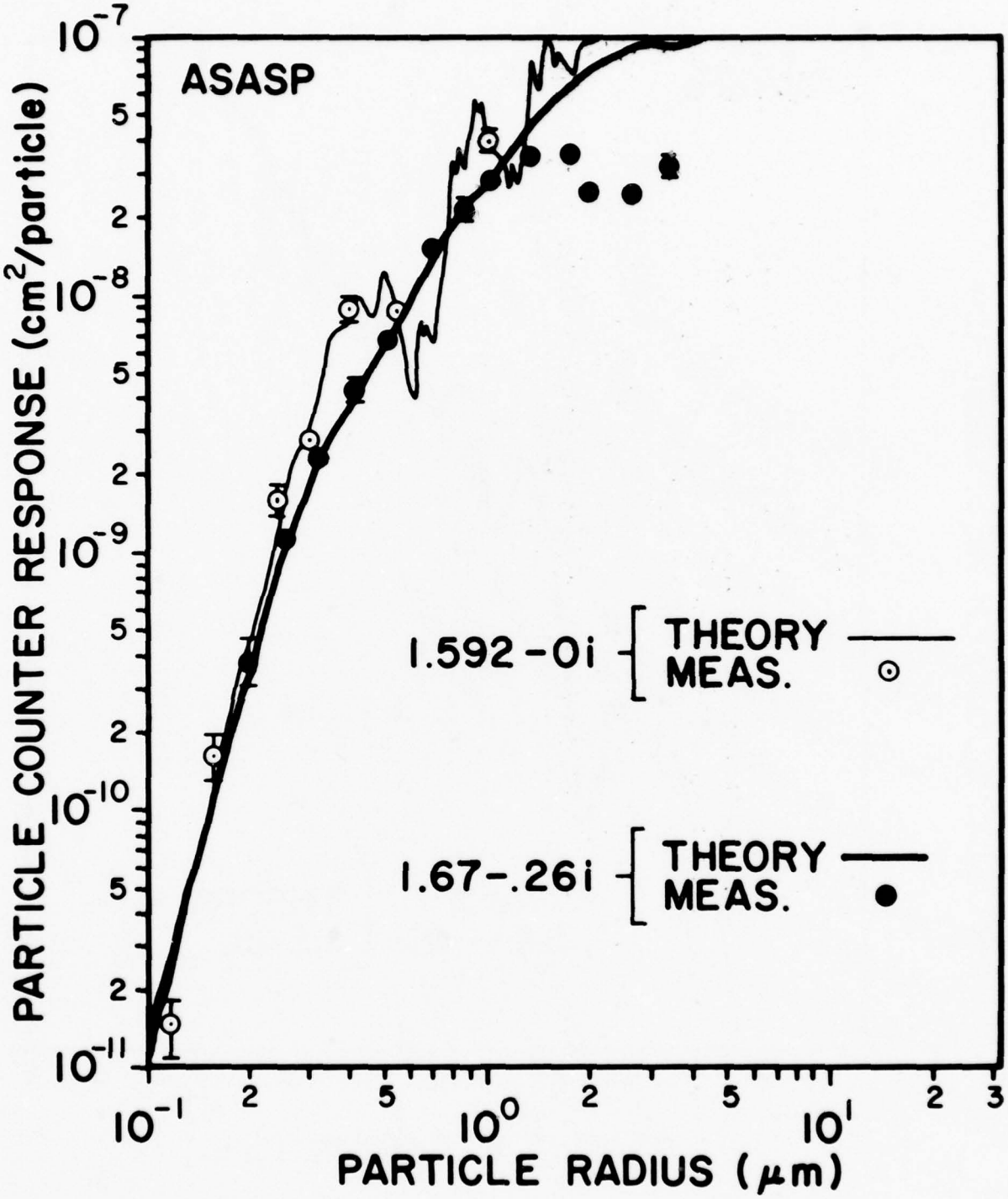

Figure 5. Knollenberg ASASP response: measured (circles) and calculated using a solution for particle scattering in a standing wave (curves) for single spherical particles versus particle size. The measurements have been normalized for best fit to the calculated response for polystyrene latex particles with refractive index m = 1.592-0i.

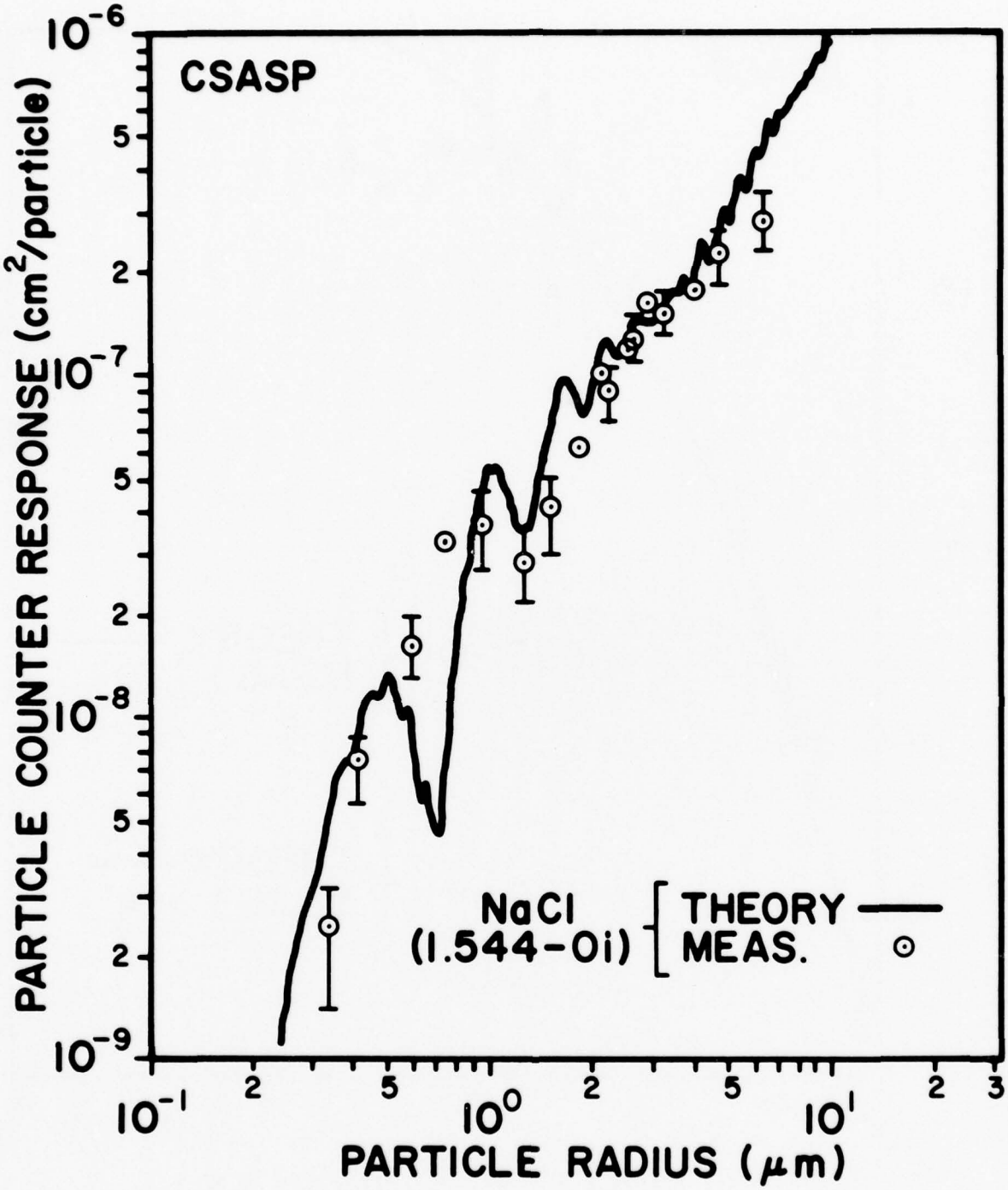

Figure 6. Knollenberg CSASP response: measured for irregular particles of sodium chloride (circles) and calculated for spheres of equal cross-sectional area using Mie scattering theory (curve) for single particles versus particle size. The measurements are relative to the polystyrene measurements which have been normalized for best fit to the calculated response for those particles (see fig. 4).

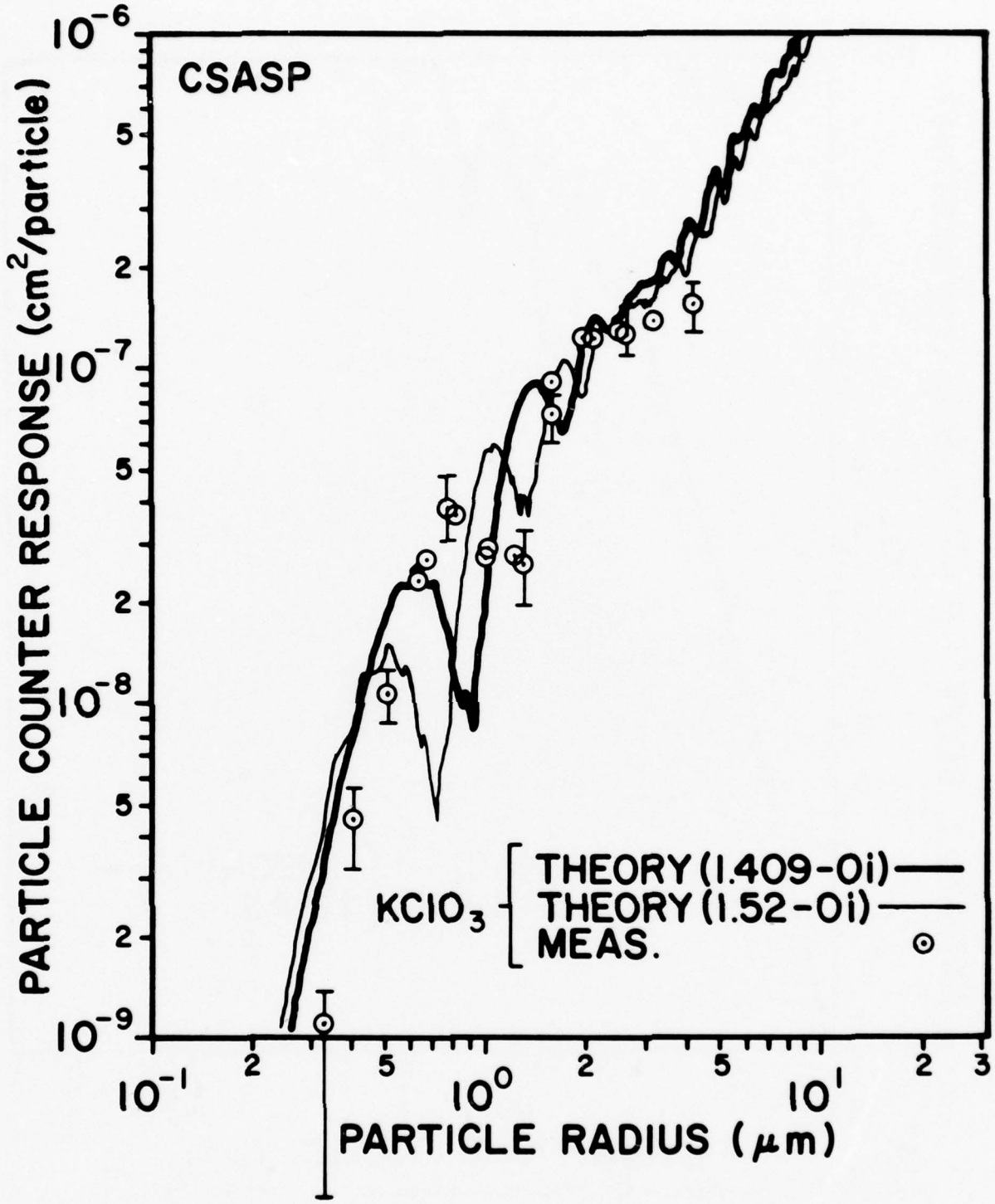

Figure 7. Same as fig. 6, except for irregular particles of potassium chlorate. Potassium chlorate is birefringent and theoretical curves are shown for particles having refractive indexes of both the ordinary (m = 1.52-0i) and extraordinary (m = 1.409-0i) waves. The measurements are relative to the polystyrene measurements which have been normalized for best fit to the calculated response for those particles (see fig. 4).

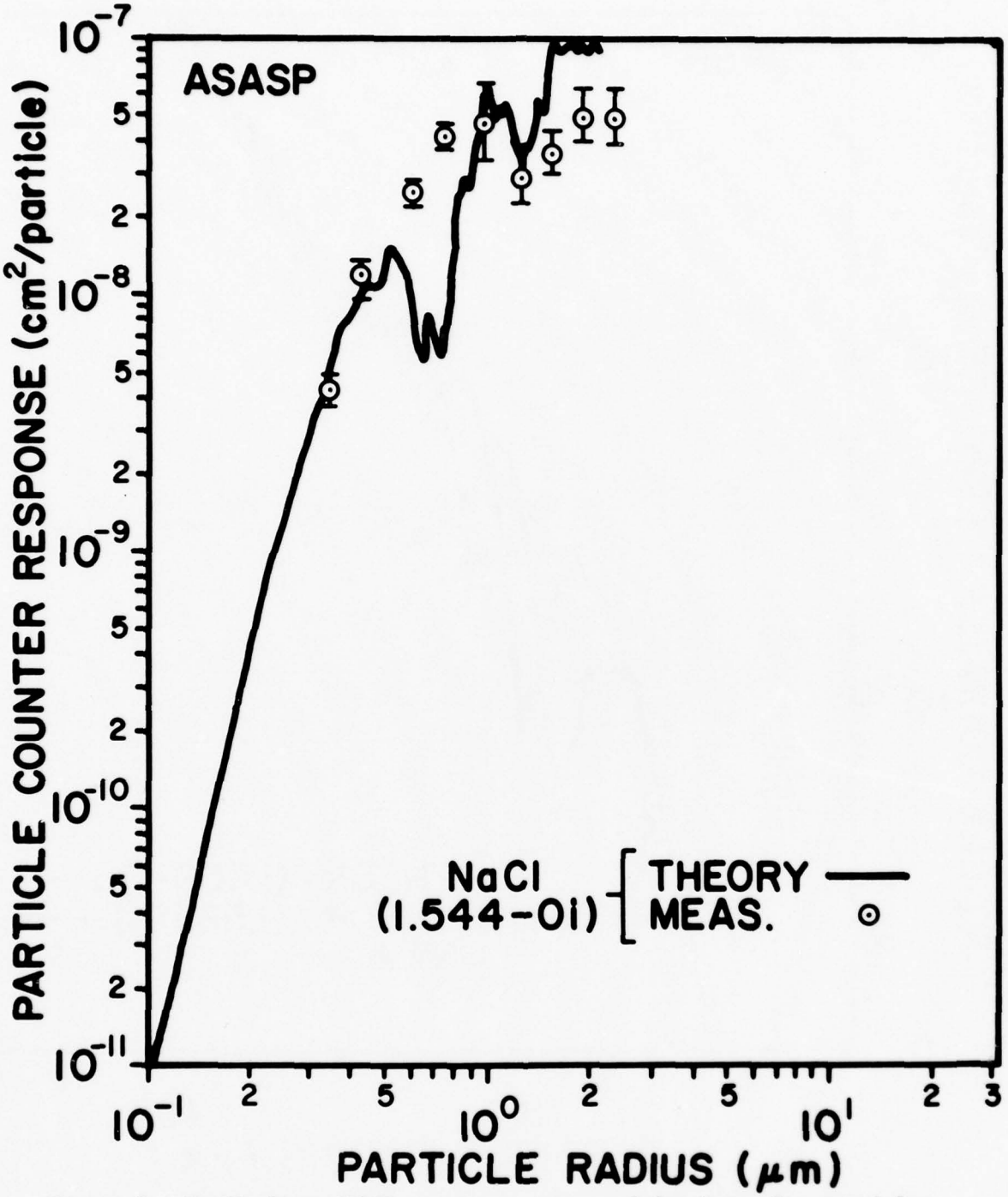

Figure 8. Knollenberg ASASP response: measured for irregular particles of sodium chloride (circles) and calculated for spheres of equal cross-sectional area using the theory for particle scattering in a standing wave (curve) for single particles versus particle size. The measurements are relative to the polystyrene measurements which have been normalized for best fit to the calculated response for those particles (see fig. 5).

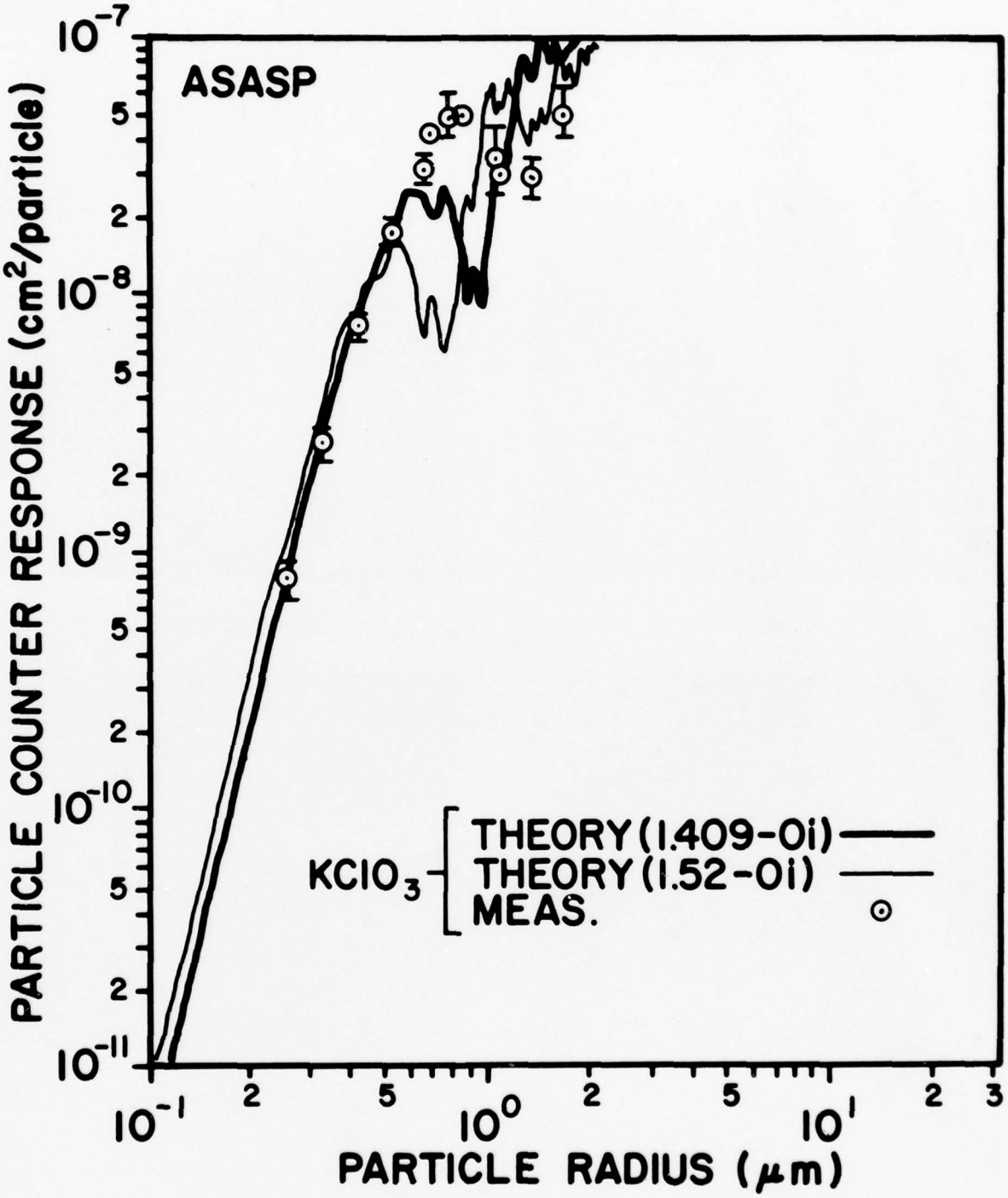

Figure 9. Same as fig. 7, except for irregular particles of potassium chlorate. Potassium chlorate is birefringent and theoretical curves are shown for particles having refractive indexes of both the ordinary (m = 1.52-0i) and extraordinary (m = 1.409-0i) waves. The measurements are relative to the polystyrene measurements which have been normalized for best fit to the calculated response for those particles (see fig. 5).

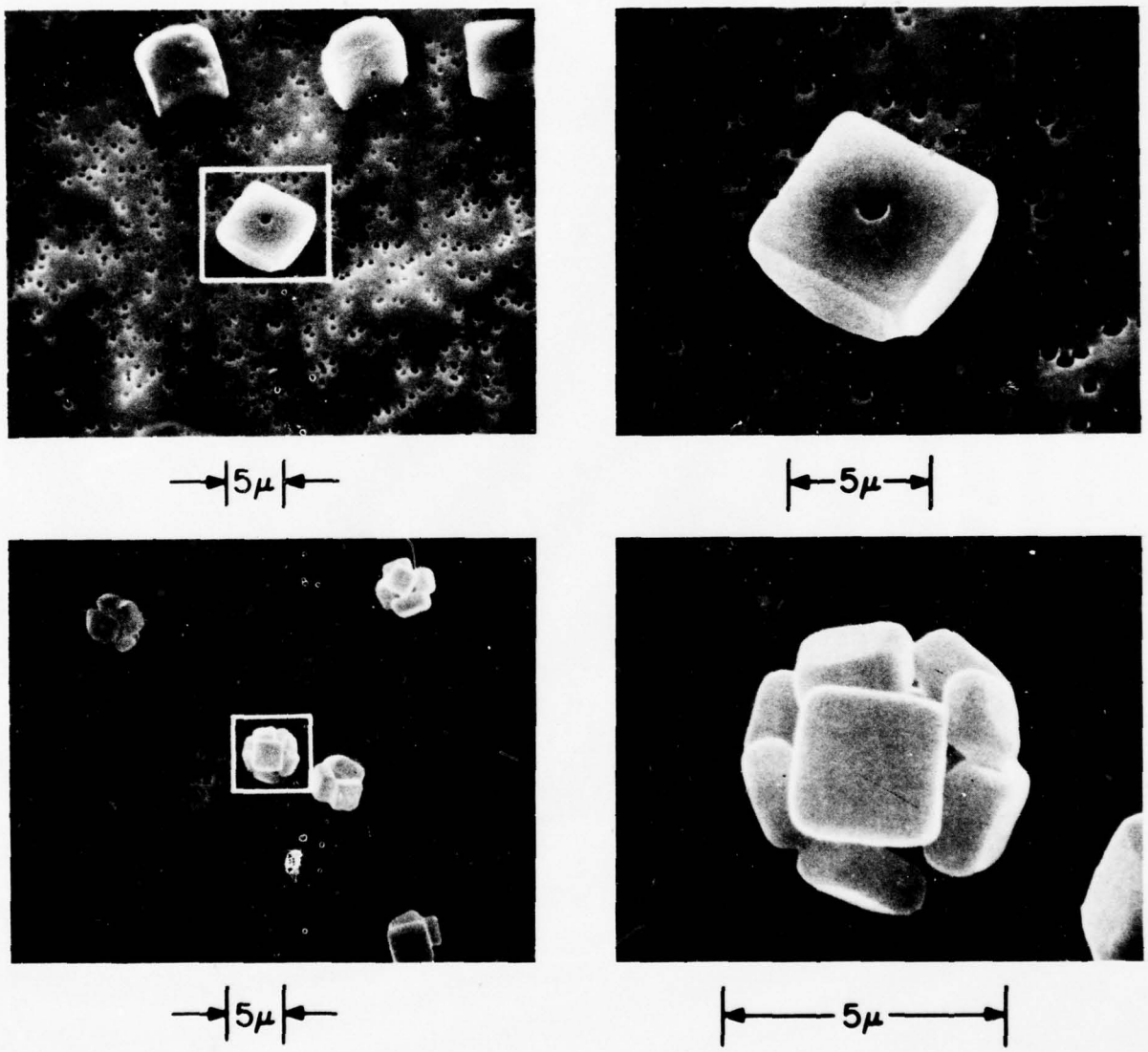

Figure 10. Scanning electron micrographs of typical monodisperse particles of sodium chloride used to measure the CSASP and ASASP response characteristics.

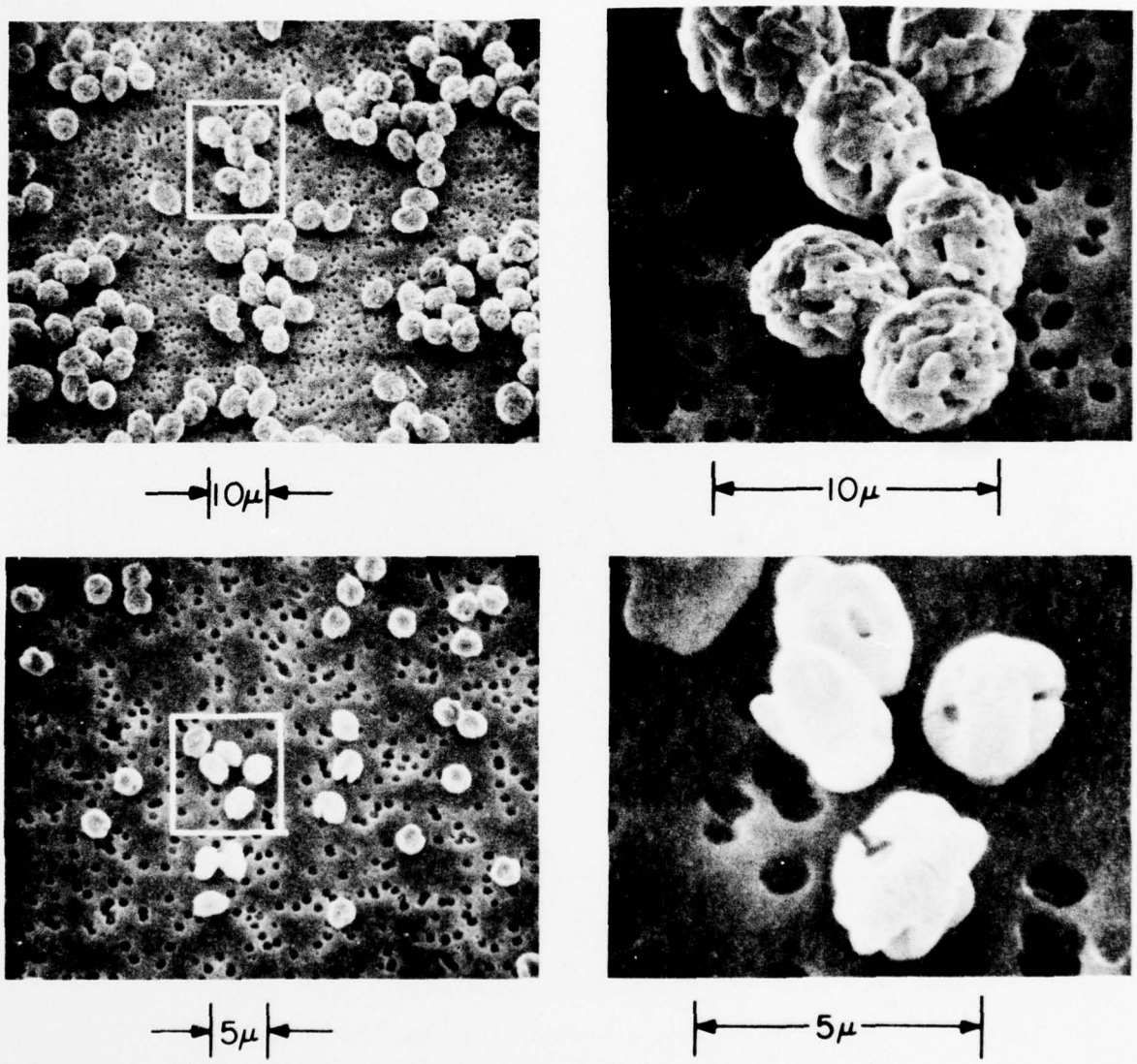

Figure 11. Scanning electron micrographs of typical monodisperse particles of potassium chlorate used to measure the CSASP and ASASP response characteristics.

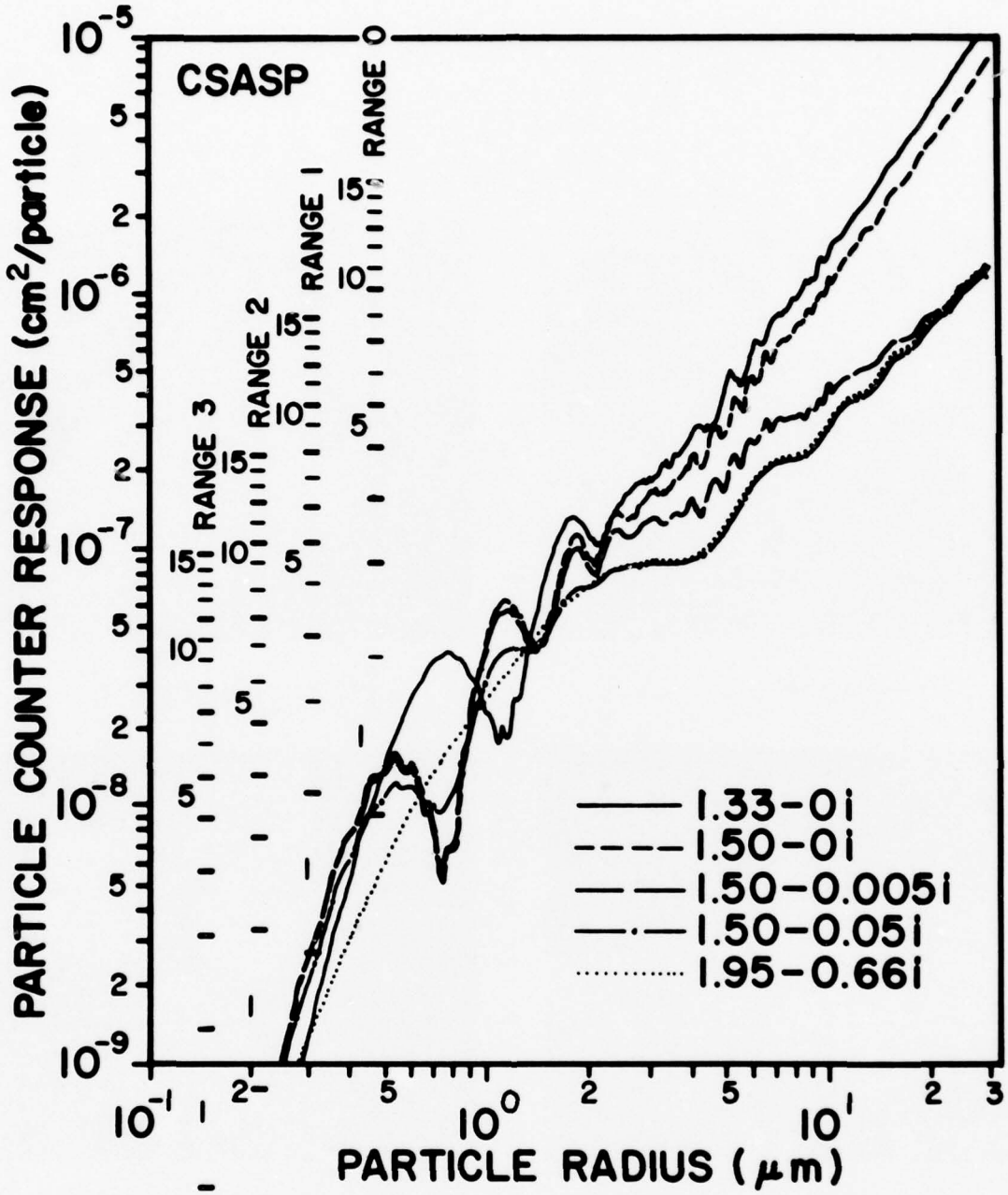

Figure 12. Mie theory response calculations for the Knollenberg CSASP particle counter for water particles with refractive index 1.33-0i, ammonium sulfate with approximate index 1.5-0i, atmospheric dust with indexes 1.50-0.005i and 1.5-0.05i, and carbon with index 1.95-0.66i. The tick marks indicate the pulse height discriminator levels as set by the manufacturer for the counter. Channels 1, 5, 10, and 15 are labeled between the appropriate tick marks for the different ranges of the instrument. The heavy tick marks indicate the pulse height discriminator levels used to avoid regions of multivalued response under the assumption that particles are water.

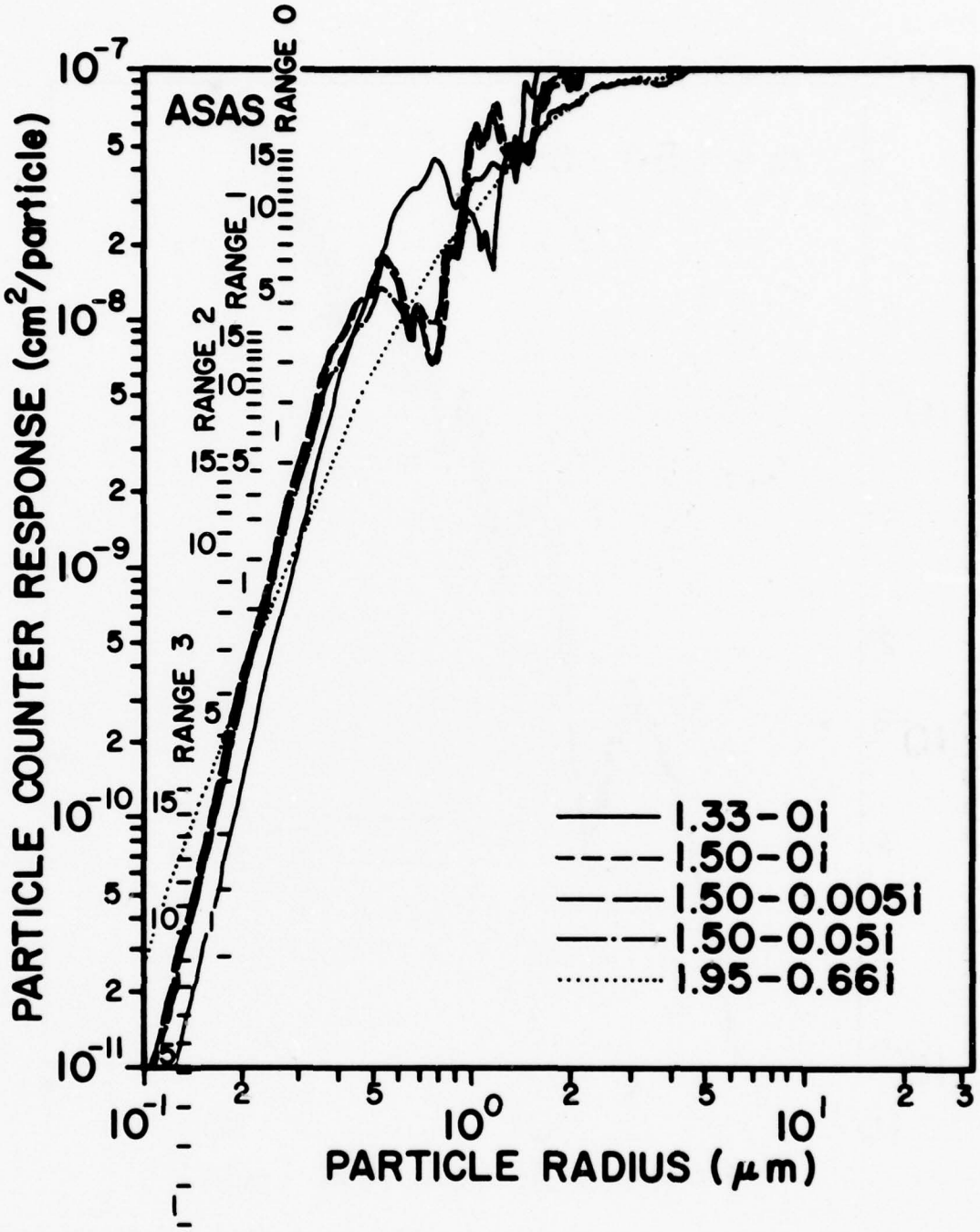

Figure 13. Response calculations for the Knollenberg ASASP particle counter using a solution for particle scattering in a standing wave for particles with refractive indexes as in fig. 12. The tick marks indicate the pulse height discriminator levels as set by the manufacturer for the counter. Channels 1, 5, 10, and 15 are labeled between the appropriate tick marks for the different ranges of the instrument.

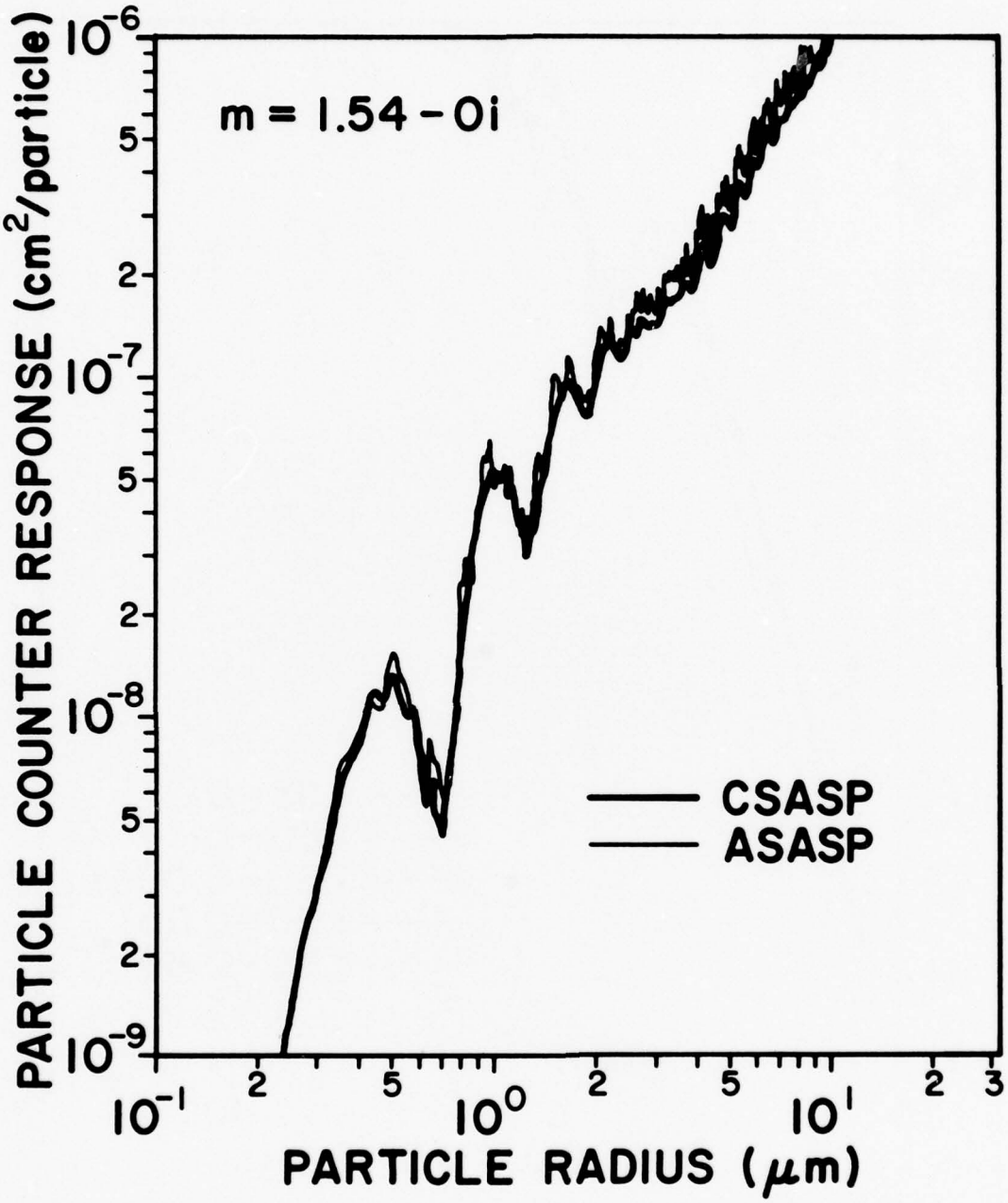

Figure 14. A comparison of response calculations for the Knollenberg CSASP and ASASP particle counters for refractive index m = 1.54-0i. The differences are a result of using Mie theory (for the CSASP) and using a theory for particle scattering in a standing wave (for the ASASP) for calculation of the response.

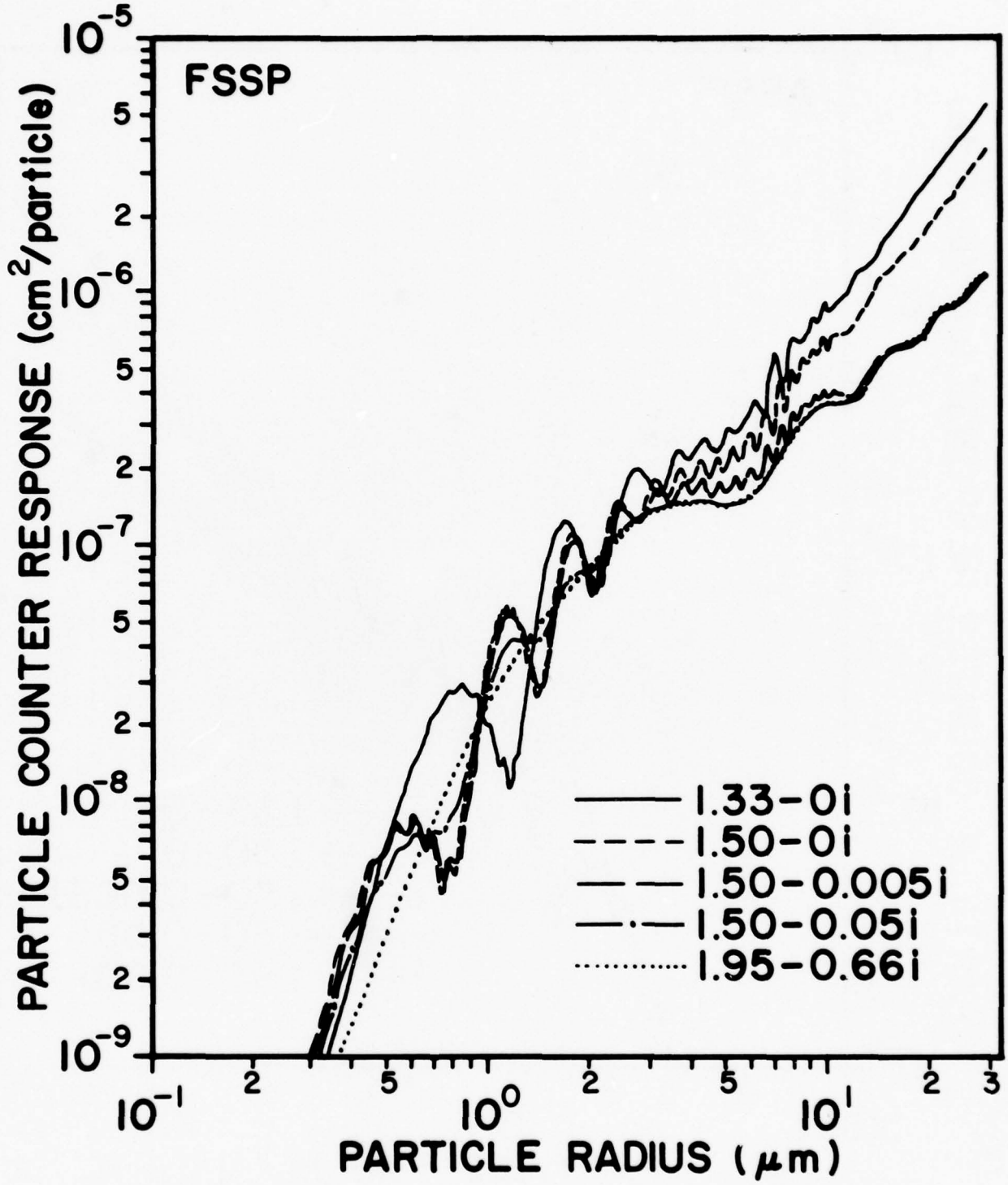

Figure 15. Mie theory response calculations for the Knollenberg FSSP particle counter for particles with refractive indexes as in fig. 12.

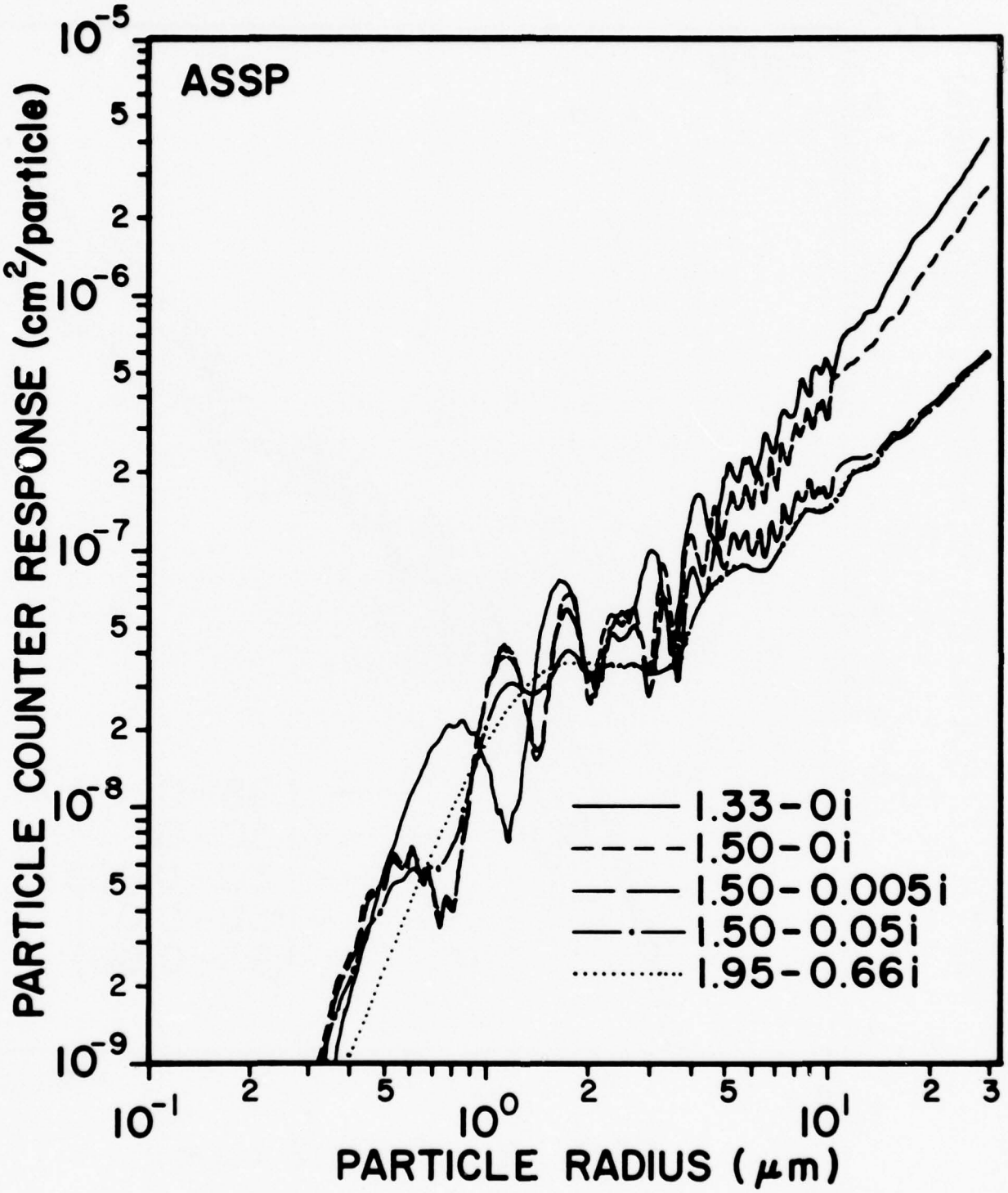

Figure 16. Mie theory response calculations for the Knollenberg ASSP particle counter for particles with refractive indexes as in fig. 12.

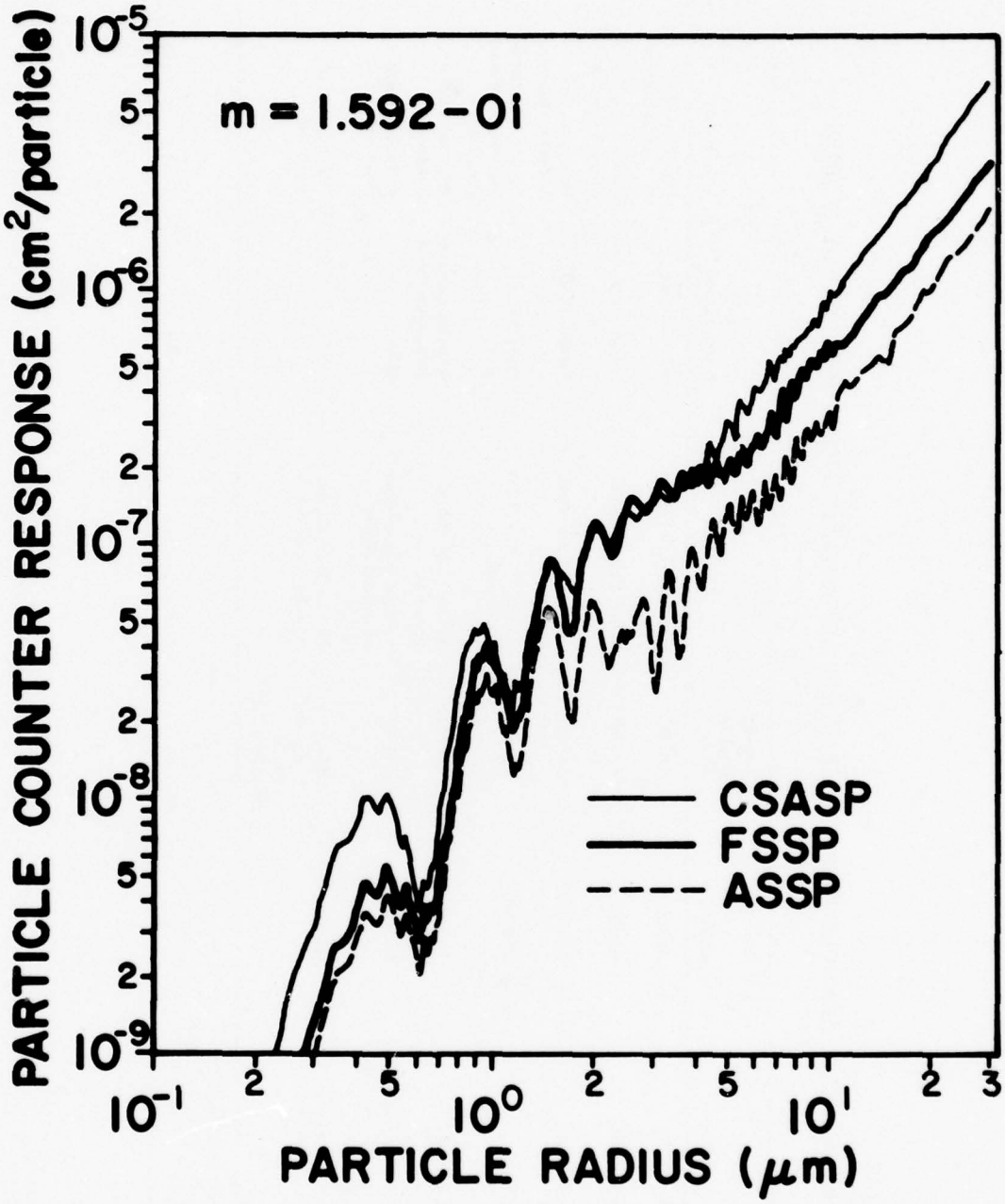

Figure 17. Response calculations for the Knollenberg CSASP, FSSP, and ASSP particle counters for latex particles having refractive index m = 1.592-0i. These curves may be used to infer positions of pulse height discriminator levels (as set by the manufacturer) relative to other theoretical response curves presented in previous figures.

TABLE 1. MONODISPERSE AEROSOLS USED IN THE CSASP AND ASASP RESPONSE MEASUREMENT STUDIES

Type	Shape	Isotropic or anisotropic	Complex refractive index	Size(s)	Size determination	Source
Polystyrene latex	spherical	isotropic	1.592-0i*	6 sizes, 0.12–0.545 μm in radius	manufacturer	Dow Chemical Midland, Michigan
Polyvinyltoluene latex	spherical	isotropic	1.581-0i*	1 size, 1.01 μm radius	manufacturer	Dow Chemical Midland, Michigan
Styrene divinylbenzene latex	spherical	isotropic	1.587-0i‡	1 size, 2.85 μm mean radius	manufacturer	Dow Chemical Midland, Michigan
Sodalime crown glass beads	spherical	isotropic	1.51-0i*	2 sizes, 5.5 and 10 μm mean radii	manufacturer	Particle Information Services Inc., Grants Pass, Oregon
Nigrosin dye	spherical	isotropic	1.67-0.26i†	13 sizes, 0.20–3.4 μm in radius	scanning electron microscope (SEM)	Vibrating Orifice Generator
Sodium chloride	cubes or assemblies of cubes with hollow centers	isotropic	1.544-0i*	17 sizes, 0.34–6.54 μm equivalent radius	SEM	Vibrating Orifice Generator
Potassium chlorate	ellipsoids with hollow centers	anisotropic	1.52-0i ordinary ray* 1.409-0i extraordinary ray*	20 sizes, 0.25–4.2 μm equivalent radius	SEM	Vibrating Orifice Generator

* Measured at $\lambda = 0.5893$ μm (sodium light).
† Measured at $\lambda = 0.6328$ μm (He Ne laser light).
‡ Measured at $\lambda = 0.5400$ μm.

TABLE 2. CHARACTERISTICS OF KNOLLENBERG LIGHT SCATTERING AEROSOL COUNTERS

Instrument	Light source	Light-collecting optics* α–β	Flow rate or active area
CSASP	5 mW He–Ne laser	4–22°	0.15 cm^3/sec
ASASP	2 mW He–Ne laser (intra-cavity)	4–22°	0.1 cm^3/sec
FSSP	5 mW He–Ne laser	3–13°	0.25 mm^2†
ASSP‡	5 mW He–Ne laser	5.3–12.4°	0.4 mm^2†

* All instruments have axial symmetry with respect to the direction of the laser source and the polar angles α, β refer to a cone subtending angles α through β from the direction of forward scattering.

† Flow rate can be determined from active area by multiplying by the speed at which air (containing aerosol) passes through the instrument.

‡ The manufacturer has produced two models of the ASSP having different optics, but only one of these has been studied here. The other collects light scattered 6.7°–14.4° from the direction of forward scattering.

TABLE 3. PARTICLE SIZE CHANNEL WIDTHS (RADII IN MICROMETERS) FOR THE KNOLLENBERG CSASP LIGHT SCATTERING AEROSOL COUNTER (a) AS SPECIFIED BY PMS AND (b) PRESENT WORK, UNDER THE ASSUMPTION PARTICLES ARE WATER DROPLETS

Channel	Instrument range							
	0		1		2		3	
	a	b	a	b	a	b	a	b
1	1.00–1.44	0.45–	0.50–0.73	0.34–0.47	0.25–0.37	0.27–0.35	0.22–0.28	0.23–0.30
2	1.44–2.08	–1.50	0.73–1.03	0.47–	0.37–0.51	0.35–0.42	0.28–0.36	0.30–0.35
3	2.08–2.90	1.50–2.50	1.03–1.39	–1.30	0.51–0.68	0.42–0.48	0.36–0.44	0.35–0.40
4	2.90–3.82	2.5–3.75	1.39–1.82	1.30–	0.68–0.86	0.48–0.55	0.44–0.54	0.40–0.44
5	3.82–4.83	3.75–4.7	1.82–2.31	–1.55	0.86–1.06	0.55–	0.54–0.64	0.44–0.48
6	4.83–5.92	4.7–	2.31–2.86	1.55–2.4	1.06–1.28	–	0.64–0.76	0.48–
7	5.92–7.05	–6.0	2.86–3.47	2.4–	1.28–1.52	–1.35	0.76–0.88	–0.56
8	7.05–8.22	6.0–	3.47–4.14	–3.6	1.52–1.77	1.35–	0.88–1.01	0.56–
9	8.22–9.39	–8.0	4.14–4.86	3.6–	1.77–2.05	–	1.01–1.14	–
10	9.39–10.56	8.0–	4.86–5.63	–4.7	2.05–2.34	–1.55	1.14–1.29	–
11	10.56–11.7	–	5.63–6.43	4.7–	2.34–2.64	1.55–	1.29–1.44	–1.35
12	11.7–12.84	–11.0	6.43–7.27	–5.6	2.64–2.97	–2.4	1.44–1.61	1.35–
13	12.84–13.9	11.0–	7.27–8.15	5.6–	2.97–3.31	2.4–	1.61–1.78	–
14	13.9–15.0	–	8.15–9.06	–	3.31–3.67	–	1.78–1.96	–
15	15.0–16.0	–14	9.06–10.0	–7.0	3.67–4.04	–3.4	1.96–2.15	–1.52

TABLE 4. SUMMARY OF FINDINGS OF RESPONSE CHARACTERISTICS OF KNOLLENBERG LIGHT-SCATTERING AEROSOL COUNTERS

Instrument	Manufacturer specifications: size range and resolution	Manufacturer recommended use*	Findings (this work): size range and resolution		
			homogeneous spherical aerosols of uniform composition	homogeneous spherical aerosols of mixed and unknown composition	irregular particles
CSASP	Size range: 0.22–16 μm radius. Resolution: ± 5% of maximum size for each range setting.	Fog, haze, dust, smoke.	Size range depends on aerosol refractive index: for water droplets (m = 1.33-0i) 0.23–14 μm, for dust (m = 1.50-0.005i) 0.21–50 μm radius. Resolution less than advertised; channels must be grouped to avoid regions of multivalued response.	Size range: 0.20–50 μm radius. Resolution severely degraded for particles with radius greater than 0.5 μm.	Size range unknown; however, slightly irregular particles have response comparable to spheres of equal area, providing equivalent radii are between 1.5 and 4 μm.
ASASP	Size range: 0.085–1.50 μm radius. Resolution: ± 5% of maximum size for each range setting.	Haze, dust, smoke.	Lower size limit depends on aerosol refractive index and is 0.096 μm radius for water droplets (m = 1.33-0i) and 0.080 μm radius for dust (m = 1.50-0.005i). Upper size limit about 1–1.5 μm radius; particles larger than 1.0 μm apparently cause reduction of laser power. Good size resolution for particles with radius less than 0.5 μm; multivalued response and generally poor resolution for larger sizes.	Size range: 0.05 μm to about 1–1.5 μm radius; see previous comment concerning particles larger than 1.0 μm radius. Relatively good resolution for particles with radius less than 0.5 μm; poor resolution for larger sizes.	Size range for slightly irregular particles about the same as for spheres of equal area. Spectra broadening significantly degrades resolution.
FSSP and ASSP	Size range: 0.22–22 μm radius. Resolution: ± 5% of maximum size for each range setting.	Fog, clouds, dust.	Size range and resolution depends on aerosol refractive index. Multivalued response for particles with radii greater than 0.5 μm. Resolution comparable to CSASP.	Resolution severely degraded for particles with radii greater than 0.5 μm.	Unknown.

* Manufacturer comments that caution should be exercised in measurement of high aerosol concentrations for all probes.

REFERENCES

1. Cooke, D. D., and M. Kerker, 1975, "Response Calculations for Light-Scattering Aerosol Particle Counters," Appl. Opt., 14:734.

2. Liu, B. Y. H., R. N. Bergland, and J. K. Agarwal, 1974, "Experimental Studies of Optical Particle Counters," Atmos. Environ., 8:717.

3. Quenzel, H., 1969, "Influence of Refractive Index on the Accuracy of Size Determination of Aerosol Particles with Light-Scattering Aerosol Counters," Appl. Opt., 8:165.

4. Quenzel, H., 1970, "Response to Comments on Influence of Refractive Index on the Accuracy of Size Determination of Aerosol Particles with Light-Scattering Aerosol Counters," Appl. Opt., 9:1931.

5. Whitby, K. T., and R. A. Vomela, 1967, "Response of Single Particle Optical Counters to Nonideal Particles," Environ. Sci. Technol., 1:801.

6. Pinnick, R. G., J. M. Rosen, and D. J. Hofmann, 1973, "Measured Light-Scattering Properties of Individual Aerosol Particles Compared to Mie Scattering Theory," Appl. Opt., 12:37.

7. Hodkinson, J. R., and J. R. Greenfield, 1965, "Response Calculations for Light-Scattering Aerosol Counters and Photometers," Appl. Opt., 4:1463.

8. Oeseburg, F., 1972, "The Influence of the Aperture of the Optical System of Aerosol Particle Counters on the Response Curve," J. Aerosol Sci., 3:307.

9. Bakhanova, R. A., and L. V. Ivanchenko, 1973, "Experimental Investigation of Scattered Luminous Flux as a Function of Drop Size in a Photoelectric Aerosol Counter," J. Aerosol Sci., 4:485.

10. Gravatt, C. C., 1973, "Real Time Measurement of the Size Distribution of Particulate Matter by a Light Scattering Method," J. A. P. C. A., 23:1035.

11. Lioy, P. J., D. Rimberg, and F. J. Haughey, 1975, "A Laser Light Scattering Particle Size Spectrometer Sensitive in the Submicron Diameter Range," J. Aerosol Sci., 6:183.

12. Heyder, J., C. Roth, and W. Stahlhofen, 1971, "A Laser Spectrometer for Size Analysis of Small Airborne Particles," J. Aerosol Sci., 2:341.

13. Gebhart, J., J. Bol, W. Heinze, and W. Letschert, 1970, "A Particle-Size Spectrometer for Aerosols Utilizing Low-Angle Scattering of Particles in a Laser Beam," Staub, 30:5.

14. Jacobi, W., J. Eichler, and N. Stolterfont, 1968, "Particle Size Spectrometry of Aerosols by Light Scattering in a Laser Beam," Staub, 28:314.

15. Bergland, R. N., and B. Y. H. Liu, 1973, "Generation of Monodisperse Aerosol Standards," Environ. Sci. Technol., 7:147.

16. Schuster, B. G., and R. Knollenberg, 1972, "Detection and Sizing of Small Particles in an Open Cavity Gas Laser," Appl. Opt., 11:1515.

17. Livingston, P. M., 1978, "Comparison of Measured 3.8-μm Scattering from Naturally Occurring Aerosols with that Predicted by Measured Particle Size Statistics," Appl. Opt., 17:818.

18. Rosen, J. M., 1968, "Simultaneous Dust and Ozone Soundings over North and Central America," J. Geophys. Res., 73:479.

ELECTRO-OPTICS DIVISION DISTRIBUTION LIST

Commander
US Army Aviation Center
ATTN: ATZQ-D-MA
Fort Rucker, AL 36362

Commander
US Army Aviation School
Fort Rucker, AL 36362

Ballistic Missile Defense Advanced
Technology Center
ATTN: ATC-R
PO Box 1500
Huntsville, AL 35807

Lockheed-Huntsville Msl & Space Co.
ATTN: Dr. Lary W. Pinkley
PO Box 1103
West Station
Huntsville, AL 35807

Chief, Atmospheric Sciences Div
Code ES-81, NASA
Marshall Space Flight Center,
AL 35812

Project Manager
Patriot Missile Systems
ATTN: DRCPM-MD-T
Redstone Arsenal, AL 35809

Commander
US Army Missile R&D Command
ATTN: DRDMI-CGA (B. W. Fowler)
Redstone Arsenal, AL 35809

Redstone Scientific Information Center
ATTN: DRDMI-TBD
US Army Missile R&D Command
Redstone Arsenal, AL 35809

Commander
US Army Missile R&D Command
ATTN: DRDMI-TEM (R. Haraway)
Redstone Arsenal, AL 35809

Commander
US Army Missile R&D Command
ATTN: DRDMI-TRA (Dr. Essenwanger)
Redstone Arsenal, AL 35809

Commander
US Army Missiles and Munitions
Center & School
ATTN: ATSIC-CD
Redstone Arsenal, AL 35809

Commander
US Army Missile R&D Command
ATTN: DRDMI-REO (Dr. Maxwell Harper)
Redstone Arsenal, AL 35809

Commander
US Army Missile R&D Command
ATTN: DRDMI-RRE (Dr. Julius Lilly)
Redstone Arsenal, AL 35809

Commander
US Army Missile R&D Command
ATTN: DRDMI-TEO (Dr. Gene Widenhofer)
Redstone Arsenal, AL 35809

Commander
US Army Missile R&D Command
ATTN: DRDMI-HRO (Dr. D.B. Guenter)
Redstone Arsenal, AL 35809

Commander
US Army Missile R&D Command
ATTN: DRDMI-TDO (Dr. Hugh Anderson)
Redstone Arsenal, AL 35809

Commander
US Army Missile R&D Command
ATTN: DRDMI-YLA (Mr. W.S. Rich)
Redstone Arsenal, AL 35809

Commander
US Army Missile R&D Command
ATTN: DRDMI-TEG (Dr. George Emmons)
Redstone Arsenal, AL 35809

Commander
HQ, Fort Huachuca
ATTN: Tech Ref Div
Fort Huachuca, AZ 85613

Commander
US Army Intelligence Center & School
ATTN: ATSI-CD
Fort Huachuca, AZ 85613

Commander
US Army Intelligence Center & School
ATTN: ATSI-CD-CS (Mr. Jim Rustenback)
Fort Huachuca, AZ 85613

Commander
US Army Intelligence Center & School
ATTN: ATSI-CD-MD
Fort Huachuca, AZ 85613

Commander
US Army Communications Command
Fort Huachuca, AZ 85613

Commander
US Army Yuma Proving Ground
ATTN: Technical Library
Bldg 2100
Yuma, AZ 85364

Northrop Corporation
Electro-Mechanical Division
ATTN: Dr. R. D. Tooley
500 East Orangethorpe Ave
Anaheim, CA 92801

Naval Weapons Center
ATTN: Code 3173 (Dr. A. Shlanta)
China Lake, CA 93555

Hughes Helicopters
ATTN: Charles R. Hill
Centinela and Teale Streets
Culter City, CA 90230

Commander
US Army Combat Dev Evaluation Command
ATTN: ATEC-PL-M (Gary Love)
Fort Ord, CA 93941

SRI International
ATTN: Dr. Ed Uthe
333 Ravenswood Avenue
Menlo Park, CA 94025

SRI International
ATTN: J. E. Van der Laan
333 Ravenswood Avenue
Menlo Park, CA 94025

Sylvania Elec Sys Western Div
ATTN: Technical Reports Library
PO Box 205
Mountain View, CA 94040

Geophysics Officer
PMTC Code 3250
Pacific Missile Test Center
Point Mugu, CA 93042

Commander
Naval Ocean Systems Center
ATTN: Code 4473 (Tech Library)
San Diego, CA 92152

Commander
Naval Ocean Systems Center
ATTN: Code 532 (Dr. Juergen Richter)
San Diego, CA 92152

General Electric -TEMPO
ATTN: Dr. James Thompson
816 State Street
PO Drawer QQ
Santa Barbara, CA 93102

The RAND Corporation
ATTN: Ralph Huschke
1700 Main Street
Santa Monica, CA 90406

National Center for Atmos Research
NCAR Library
PO Box 3000
Boulder, CO 80307

Library-R-51-Tech Reports
NOAA/ERL
320 S. Broadway
Boulder, CO 80302

Wave Propagation Laboratory
NOAA/ERL
ATTN: Dr. Vernon Derr
Boulder, CO 80302

Particle Measuring Systems, Inc.
ATTN: Dr. Robert Knollenberg
1855 South 57th Court
Boulder, CO 80301

US Department of Commerce
Institute for Telecommunication Sciences
ATTN: Dr. H. J. Liebe
Boulder, CO 80303

HQDA (SAUS-OR/Hunter Woodall)
Rm 2E614, Pentagon
Washington, DC 20301

Dr. Herbert Fallin
ODUSA-OR
Rm 2E621, Pentagon
Washington, DC 20301

COL Elbert Friday
OUSDR&E
Rm 3D129, Pentagon
Washington, DC 20301

Defense Communications Agency
Technical Library Center
Code 205
Washington, DC 20305

Director
Defense Nuclear Agency
ATTN: Technical Library
Washington, DC 20305

Director
Defense Nuclear Agency
ATTN: RAAE (MAJ Ed Mueller)
Washington, DC 20305

Director
Defense Nuclear Agency
ATTN: SPAS (Mr. A.T. Hopkins)
Washington, DC 20305

Defense Intelligence Agency
ATTN: Scientific Advisory Committee
Washington, DC 20310

HQDA (DAMA-ARZ-D/Dr. Verderame)
Washington, DC 20310

HQDA (DAMI-ISP/Mr. Beck)
Washington, DC 20310

Department of the Army
Deputy Chief of Staff for
Operations and Plans
ATTN: DAMO-RQ
Washington, DC 20310

Department of the Army
Director of Telcommunications and
Command and Control
ATTN: DAMO-TCZ
Washington, DC 20310

Department of the Army
Deputy Chief of Staff for Research,
Development and Acquisition
ATTN: DAMA-AR
Washington, DC 20310

Department of the Army
Assistant Chief of Staff for Intelligence
ATTN: DAMI-TS
Washington, DC 20310

HQDA (DAEN-RDM/Dr. de Percin)
Forrestal Building
Washington, DC 20314

Director
Naval Research Laboratory
ATTN: Code 5530
Washington, DC 20375

Director
Naval Research Laboratory
ATTN: Code 2627
Washington, DC 20375

Director
Naval Research Laboratory
ATTN: Code 1409
(Dr. J. M. MacCallum)
Washington, DC 20375

Director
Naval Research Laboratory
ATTN: Code 5567
(Dr. James A. Dowling)
Washington, DC 20375

Commander
US Army Armor Center
ATTN: ATZK-CD
Fort Knox, KY 40121

Aerodyne Research Inc.
ATTN: Dr. John Ebersole
Bedford Research Park
Crosby Drive
Bedford, MA 01730

Commander
Air Force Geophysical Laboratory
ATTN: OPI (Dr. R.A. McClatchey)
Hanscom AFB, MA 01731

Commander
Air Force Geophysical Laboratory
ATTN: OPI (Dr. R. Fenn)
Hanscom AFB, MA 01731

Commander
US Army Ordnance Center and School
ATTN: ATSL-CD
Aberdeen Proving Ground, MD 21005

Commander
US Army Ordnance & Chemical Center
and School
ATTN: ATSL-CLC (Dr. Thomas Welch)
Aberdeen Proving Ground, MD 21005

Commander
US Army Ballistic Rsch Laboratory
ATTN: Dr. Robert Eichelberge
Aberdeen Proving Ground, MD 21005

Commander
US Army Ballistic Rsch Laboratory
ATTN: Mr. Alan Downs
Aberdeen Proving Ground, MD 21005

Commander
US Army Ballistic Rsch Laboratory
ATTN: DRDAR-BLB (Mr. Arthur LaGrange)
Aberdeen Proving Ground, MD 21005

Commander
US Army Ballistic Research Laboratory
ATTN: Mr. Richard McGee
Aberdeen Proving Ground, MD 21005

Project Manager
Smoke/Obscurants
ATTN: DRDPM-SMC (COL H. Shelton)
Aberdeen Proving Ground, MD 21005

Project Manager
Smoke/Obscurants
ATTN: DRDPM-SMC (Dr. T. Van de Wal Jr.)
Aberdeen Proving Ground, MD 21005

Project Manager
Smoke/Obscurants
ATTN: DRDPM-SMC (Mr. G. Bowman)
Aberdeen Proving Ground, MD 21005

Project Manager
Smoke/Obscurants
ATTN: DRDPM-SMC (Mr. J. Steedman)
Aberdeen Proving Ground, MD 21005

Commander
US Army Test & Evaluation Command
ATTN: DRSTE-AD-M (Mr. Warren M. Baily)
Aberdeen Proving Ground, MD 21005

Director
US Army Material Systems Analysis Activity
ATTN: DRXSY-LA (Mr. Paul Frossell)
Aberdeen Proving Ground, MD 21005

Director
US Army Material Systems Analysis Activity
ATTN: DRXSY-LA (Mr. Michael Starks)
Aberdeen Proving Ground, MD 21005

Director
US Army Material Systems Analysis Activity
ATTN: DRXSY-LA (Mr. William Smith)
Aberdeen Proving Ground, MD 21005

Director
US Army Material Systems Analysis Activity
ATTN: DRXSY-LA (Dr. Keats Pullen)
Aberdeen Proving Ground, MD 21005

Director
Naval Research Laboratory
ATTN: Code 5567
(Dr. Steve Hanley)
Washington, DC 20375

Director
Naval Research Laboratory
ATTN: Code 8320
(Dr. L.H. Ruhnke)
Washington, DC 20375

The Library of Congress
ATTN: Exchange & Gift Div
Washington, DC 20540
2

Head, Atmos Rsch Section
Div Atmospheric Science
National Science Foundation
1800 G. Street, NW
Washington, DC 20550

ADTC/DLODL
Eglin AFB, FL 32542

Naval Training Equipment Center
ATTN: Technical Library
Orlando, FL 32813

Georgia Institute of Technology
ATTN: Dr. James Wiltse
Atlanta, GA 30332

Georgia Institute of Technology
ATTN: Dr. Robert McMillan
Atlanta, GA 30332

Georgia Institute of Technology
ATTN: Mr. James Gallagher
Atlanta, GA 30332

Commander
US Army Infantry Center
Fort Benning, GA 31805

Commander
US Army Infantry Center
ATTN: AT2B-CD
Fort Benning, GA 31805

US Army Signal School
ATTN: ATSN-CD
Fort Gordon, GA 30905

USAFETAC
Scott AFB, IL 62225

Commander
Air Weather Service
ATTN; DNPP (LTC Donald Hodges)
Scott AFB, IL 62269

Commander
US Army Combined Arms Center
ATTN: ATCA-CAA-Q (Kent Pickett)
Fort Leavenworth, KS 66027

Commander
US Army Combined Arms Center
ATTN: ATCA-CS
Fort Leavenworth, KS 66027

Commander
US Army Combined Arms Center
ATTN: ATCA-CCC
Fort Leavenworth, KS 66027

Commander
US Army Combined Arms Center
ATTN: ATCA-CDC
Fort Leavenworth, KS 66027

Commander
US Army Combined Arms Center
ATTN: ATCA-CDE
Fort Leavenworth, KS 66027

Commander
US Army Combined Arms Center
ATTN: ATCA-CCM
Fort Leavenworth, KS 66027

Commander
US Army Armor Center
ATTN: ATZK-AE-TA
(Dr. Charles Leake)
Fort Knox, KY 40121

Director
US Army Material Systems Analysis Activity
ATTN: DRXSY-GI (Mr. Sid Geraud)
Aberdeen Proving Ground, MD 21005

Director
US Army Armament R&D Command
Chemical Systems Laboratory
ATTN: DRDAR-CLB-PS (Dr. Ed Stuebing)
Aberdeen Proving Ground, MD 21010

Director
US Army Armament R&D Command
Chemical Systems Laboratory
ATTN: DRDAR-CLB-PS (Mr. Joseph Vervier)
Aberdeen Proving Ground, MD 21010

Director
US Army Armament R&D Command
Chemical Systems Laboratory
ATTN: DRDAR-CLY-A (Mr. Ron Pennsyle)
Aberdeen Proving Ground, MD 21010

Commander
Harry Diamond Laboratories
ATTN: Dr. William Carter
2800 Powder Mill Road
Adelphi, MD 20783

Commander
Harry Diamond Laboratories
ATTN: DELHD-RAC (Dr. R.G. Humphrey)
2800 Powder Mill Road
Adelphi, MD 20783

Commander
Harry Diamond Laboratories
ATTN: Dr. Ed Brown
2800 Powder Mill Road
Adelphi, MD 20783

Commander
Harry Diamond Laboratories
ATTN: Dr. Stan Kulpa
2800 Powder Mill Road
Adelphi, MD 20783

Commander
ERADCOM
ATTN: DRDEL-AP
2800 Powder Mill Road
Adelphi, MD 20783
2

Commander
ERADCOM
ATTN: DRDEL-CG/DRDEL-DC/DRDEL-CS
2800 Powder Mill Road
Adelphi, MD 20783

Commander
ERADCOM
ATTN: DRDEL-CT
2800 Powder Mill Road
Adelphi, MD 20783

Commander
ERADCOM
ATTN: DRDEL-EA
2800 Powder Mill Road
Adelphi, MD 20783

Commander
ERADCOM
ATTN: DRDEL-PA/DRDEL-ILS/DRDEL-E
2800 Powder Mill Road
Adelphi, MD 20783

Commander
ERADCOM
ATTN: DRDEL-PAO (S. Kimmel)
2800 Powder Mill Road
Adelphi, MD 20783

Commander
ERADCOM
ATTN: DRDEL-PAO (Paul Case)
2800 Powder Mill Road
Adelphi, MD 20783

Commander
HQ, AFSC/DLCAA
ATTN: LTC Glen Warner
Andrews AFB, MD 20334

AFSC
ATTN: WER (Mr. Richard F. Picanso)
Andrews AFB, MD 20334

Commander
Concepts Analysis Agency
ATTN: MOCA-SMC (Hal E. Hock)
8120 Woodmont Ave
Bethesda, MD 20014

Martin Marietta Laboratories
ATTN: Jar Mo Chen
1450 South Rolling Road
Baltimore, MD 21227

Commander
US Army Intelligence Agency
Fort George G. Meade, MD 20755

Director
National Security Agency
ATTN: R52/Woods
Fort George G. Meade, MD 20755

Chief
Intelligence Materiel Dev & Support Ofc
ATTN: DELEW-WL-I
Bldg 4554
Fort George G. Meade, MD 20755

Acquisitions Section, IRDB-D823
Library & Info Service Div, NOAA
6009 Executive Blvd
Rockville, MD 20852

Naval Surface Weapons Center
ATTN: Code WR42 (Dr. Barry Katz)
White Oak Library
Silver Spring, MD 20910

The Environmental Research
Institute of MI
ATTN: IRIA Library
PO Box 8618
Ann Arbor, MI 48107

Science Applications Inc.
ATTN: Dr. Robert E. Meredith
15 Research Drive
PO Box 7329
Ann Arbor, MI 48107

Science Applications Inc.
ATTN: Dr. Robert E. Turner
15 Research Drive
PO Box 7329
Ann Arbor, MI 48107

Commander
US Army Tank-Automative R&D Command
Warren, MI 48090

Dr. A. D. Belmont
Research Division
PO Box 1249
Control Data Corp
Minneapolis, MN 55440

Commander
US Army Aviation Systems Command
St. Louis, MO 63166

Director
Naval Oceanography & Meteorology
NSTL Station
Bay St Louis, MS 39529

Director
US Army Engr Waterways Experiment Sta
ATTN: Library
PO Box 631
Vicksburg, MS 39180

Director
US Army Engr Waterways Experiment Sta
ATTN: WESFT (Dr. Bob Penn)
PO Box 631
Vicksburg, MS 39180

Director
US Army Engr Waterways Experiment Sta
ATTN: WESFT (Mr. Jerry Lundien)
PO Box 631
Vicksburg, MS 39180

US Army Research Office
ATTN: DRXRO-PP
PO Box 12211
Research Triangle Park, NC 27709

US Army Research Office
ATTN: DRXRO-GS (Dr. Arthur V. Dodd)
PO Box 12211
Research Triangle Park, NC 27709

Commander
US Army Cold Regions Rsch & Engr Lab
ATTN: Mr. Roger Berger
Hanover, NH 03755

Commander
US Army Cold Regions Rsch & Engr Lab
ATTN: Mr. George Aitken
Hanover, NH 03755

Commander
US Army Cold Regions Rsch & Engr Lab
ATTN: CRREL-RD (Dr. K.F. Sterrett)
Hanover, NH 03755

Commander
US Army Armament R&D Command
ATTN: DRDAR-TSS (Bldg 59)
Dover, NJ 07801

Commander
US Army Armament R&D Command
ATTN: DRDAR-AC (J. Greenfield)
Dover, NJ 07801

Project Manager
Cannon Artillery Weapons Systems
ATTN: DRCPM-CAWS
Dover, NJ 07801

Project Manager
Cannon Artillery Weapons Systems
ATTN: DRCPM-CAWS-GP (G.H. Waldron)
Dover, NJ 07801

Commander
HQ, US Army Avionics R&D Activity
ATTN: DAVAA-O
Fort Monmouth, NJ 07703

Commander/Director
US Army Combat Surveillance & Target
Acquisition Laboratory
ATTN: DELCS-D
Fort Monmouth, NJ 07703

Director
US Army Electronics Technology &
Devices Laboratory
ATTN: DELET-D
Fort Monmouth, NJ 07703

Commander
US Army Electronic Warfare Laboratory
ATTN: DELEW-D (Mr. George Haber)
Fort Monmouth, NJ 07703

Commander
US Army Night Vision &
Electro-Optics Laboratory
ATTN: DELNV-L (Dr. Rudolf Buser)
Fort Monmouth, NJ 07703

Commander
US Army Night Vision &
Electro-Optics Laboratory
ATTN: DELNV-L (Dr. Robert Rodhe)
Fort Monmouth, NJ 07703

Commander
ERADCOM Technical Support Activity
ATTN: DELSD-L
Fort Monmouth, NJ 07703

Project Manager, FIREFINDER
ATTN: DRCPM-FF
Fort Monmouth, NJ 07703

Project Manager, REMBASS
ATTN: DRCPM-RBS
Fort Monmouth, NJ 07703

Commander
US Army Satellite Comm Agency
ATTN: DRCPM-SC-3
Fort Monmouth, NJ 07703

Commander
ERADCOM Scientific Advisor
ATTN: DRDEL-SA
Fort Monmouth, NJ 07703

Project Manager
Army Tactical Data Systems
ATTN: DRCPM-TDS
Fort Monmouth, NJ 07703

6585 TG/WE
Holloman AFB, NM 88330

AFWL/WE
Kirtland, AFB, NM 87117

AFWL/Technical Library (SUL)
Kirtland AFB, NM 87117

Commander
US Army Test & Evaluation Command
ATTN: STEWS-AD-L
White Sands Missile Range, NM 88002

Chief
US Army Electronics R&D Command
Office of Missile Electronic Warfare
ATTN: DELEW-M-STE (Dr. Steven Kovel)
White Sands Missile Range, NM 88002

US Army Office of the Test Director
Joint Services EO GW CM Test Program
ATTN: DRXDE-TD (Mr. Weldon Findley)
White Sands Missile Range, NM 88002

Commander
TRASANA
ATTN: ATAA-D (Dr. Wilbur Payne)
White Sands Missile Range, NM 88002

Commander
TRASANA
ATTN: ATAA-TDB (Louis Dominquez)
White Sands Missile Range, NM 88002

Commander
TRASANA
ATTN: ATAA-PL (Dolores Anguiano)
White Sands Missile Range, NM 88002

Commander
TRASANA
ATTN: ATAA-TOP (Roger Willis)
White Sands Missile Range, NM 88002

Commander
TRASANA
ATTN: ATAA-TGC (Dr. Alfonso Diaz)
White Sands Missile Range, NM 88002

Commander
TRASANA
ATTN: ATAA-TGA (Mr. Edward Henry)
White Sands Missile Range, NM 88002

Grumman Aerospace Corporation
Research Dept - MS A08-35
ATTN: John E. A. Selby
Bethpage, NY 11714

Rome Air Development Center
ATTN: Documents Library
TSLD (Bette Smith)
Griffiss AFB, NY 13441

Commander
US Army Tropic Test Center
ATTN: STETC-TD (Info Center)
APO New York 09827

Commander
US Army R&D Coordinator
US Embassy, Bonn, Box 165
APO New York 09080

HQ
USAREUR & Seventh Army
APO New York, NY 09403

Air Force Avionics Laboratory
ATTN: AFAL/RWI-3 (Cpt James Pryce)
Wright-Patterson AFB, OH 45433

Air Force Air Systems Laboratory
ATTN: AFAL/RWI-e (Dr. George Mavko)
Wright-Patterson AFB, OH 45433

Commandant
US Army Field Artillery School
ATTN: ATSF-CD-R (Mr. Farmer)
Fort Sill, OK 73503

Commandant
US Army Field Artillery School
ATTN: ATSF-CF-R
Fort Sill, OK 73503

Director CFD
US Army Field Artillery School
ATTN: Met Division
Fort Sill, OK 73503

Commandant
US Army Field Artillery School
ATTN: Morris Swett Library
Fort Sill, OK 73503

Commander
US Army Combined Arms Center
ATTN: ATCA-CAT-V (R. DeKinder, Jr.)
Fort Sill, OK 73503

US Army Field Artillery School
ATTN: ATSF-CD
Fort Sill, OK 73503

Commander
273rd Transportation Company
(Heavy Helicopter)
W44CCQ
ATTN: CW4 J. Kard
Fort Sill, OK 73503

Commander
Naval Air Development Center
ATTN: Code 202 (Mr. Thomas Shopple)
Warminster, PA 18974

University of Texas at El Paso
Electrical Engineering Department
ATTN: Dr. Joseph H. Pierluissi
El Paso, TX 79968

US Army Air Defense School
ATTN: ATSA-CD
Fort Bliss, TX 79916

Commander
3rd Armored Cavalry Regiment
ATTN: AFVF-SO
Fort Bliss, TX 79916

Commander
TRADOC Combined Arms Test Activity
ATTN: ATCAT-OP-Q (Wayland Smith)
Fort Hood, TX 76544

Commander
TRADOC Combined Arms Test Activity
ATTN: Technical Library
Fort Hood, TX 76544

Commander
TRADOC Combined Arms Test Activity
ATTN: ATCAT-SCI (Darrell Collin)
Fort Hood, TX 76544

MAJ Joseph Caruso
HQ, TRADOC Combined Arms Test Activity
ATTN: ATCAT-CA
Fort Hood, TX 76544

Commandant
US Army Air Defense School
ATTN: Mr. Blanchett
Fort Bliss, TX 79916

Commander
US Army Dugway Proving Ground
ATTN: STEDP-MT-DA-L
Dugway, UT 84022

Commander
US Army Dugway Proving Ground
ATTN: STEDP-MT-DA-S (John Treatheway)
Dugway, UT 84022

Commander
US Army Dugway Proving Ground
ATTN: STEDP-MT-DA-M (Paul Carlson)
Dugway, UT 84022

Commander
US Army Dugway Proving Ground
ATTN: STEDP-MT-DA-T (William Peterson)
Dugway, UT 84022

Defense Documentation Center
ATTN: DDC-TCA
Cameron Station Bldg 5
Alexandria, VA 22314
12

Ballistic Missile Defense Program Office
ATTN: DACS-BMT
5001 Eisenhower Avenue
Alexandria, VA 22333

Commander
US Army Materiel Dev & Readiness Command
ATTN: DRCLDC (Mr. James Bender)
5001 Eisenhower Ave
Alexandria, VA 22333

Commander
US Army Materiel Dev & Readiness Command
ATTN: DRCBSI
5001 Eisenhower Ave
Alexandria, VA 22333

Institute for Defense Analysis
ATTN: Mr. Lucian Biberman
Arlington, VA 22202

Institute for Defense Analysis
ATTN: Dr. Robert Roberts
Arlington, VA 22202

Director
ARPA
1400 Wilson Blvd
Arlington, VA 22209

Defense Advanced Rsch Projects Agency
ATTN: Steve Zakanyez
1400 Wilson Blvd
Arlington, VA 22209

Defense Advanced Rsch Projects Agency
ATTN: Dr. Carl Thomas
1400 Wilson Blvd
Arlington, VA 22209

Defense Advanced Rsch Projects Agency
ATTN: Dr. James Tegnelia
1400 Wilson Blvd
Arlington, VA 22209

Commander
US Army Security Agency
ATTN: IARD-MF
Arlington Hall Station
Arlington, VA 22212

USA Intelligence & Security Command
ATTN: E. A. Speakman,
Science Advisor
Arlington Hall Station
Arlington, VA 22212

Commander
US Army Foreign Sci & Tech Center
ATTN: DRXST-IS1
220 7th Street, NE
Charlottesville, VA 22901

Commander
US Army Foreign Sci & Tech Center
ATTN: Dr. Orville Harris
220 7th Street, NE
Charlottesville, VA 22901

Commander
US Army Foreign Sci & Tech Center
ATTN: Dr. Bertram Smith
220 7th Street, NE
Charlottesville, VA 22901

Naval Surface Weapons Center
ATTN: Code G65
Dahlgren, VA 22448

Commander
Operational Test & Evaluation Agency
Columbia Pike Bldg
5600 Columbia Pike
Falls Church, VA 22041

Commander
US Army Night Vision
& Electro-Optics Lab
ATTN: DELNV-D (Mr. John Johnson)
Fort Belvoir, VA 22060

Commander
US Army Night Vision
& Electro-Optics Lab
ATTN: DELNV-VI (Mr. J.R. Moulton)
Fort Belvoir, VA 22060

Commander
US Army Night Vision
& Electro-Optics Lab
ATTN: DELNV-VI (Luanne Overt)
Fort Belvoir, VA 22060

Commander
US Army Night Vision
& Electro-Optics Lab
ATTN: DELNV-VI (Tom Cassidy)
Fort Belvoir, VA 22060

Commander
US Army Night Vision
& Electro-Optics Lab
ATTN: DELNV-VI (Richard Bergemann)
Fort Belvoir, VA 22060

Commander
US Army Night Vision
& Electro-Optics Lab
ATTN: DELNV-VI (Dr. John Ratches)
Fort Belvoir, VA 22060

Commander
US Army Night Vision
& Electro-Optics Lab
ATTN: DELNV-FIR (Fred Petito)
Fort Belvoir, VA 22060

Commander
US Army Engineering Topographic Lab
ATTN: ETL-TD-MB
Fort Belvoir, VA 22060

US Army Engineer School
ATTN: ATSE-CD
Fort Belvoir, VA 22060

Commandant
US Army Engineering Center & School
Directorate of Combat Developments
Fort Belvoir, VA 22060

Commander
US Army Mobility Equip R&D Command
ATTN: DRDME-RT (Mr. Fred Kezer)
Fort Belvoir, VA 22060

Director
Applied Technology Laboratory
ATTN: DAVDL-EU-TSD (Tech Library)
Fort Eustis, VA 23604

Department of the Air Force
OL-C, 5WW
Fort Monroe, VA 23651

Commander
HQ, TRADOC
ATTN: ATCD-PM
Fort Monroe, VA 23651

Commander
US Army Training & Doctrine Command
Fort Monroe, VA 23651

Commander
US Army Training & Doctrine Command
ATTN: ATCD-IE-R (Mr. Dave Ingram)
Fort Monroe, VA 23651

Commander
US Army Training & Doctrine Command
ATTN: ATCD-STE
Fort Monroe, VA 23651

Commander
US Army Training & Doctrine Command
ATTN: ATCD-CF (Chris O'Conner)
Fort Monroe, VA 23651

Commander
US Army Training & Doctrine Command
ATTN: ATCD-AN-TD (Seymour Goldbert)
Fort Monroe, VA 23651

Commander
US Army Training & Doctrine Command
ATTN: ATCD-TA (M. P. Pastel)
Fort Monroe, VA 23651

Commander
US Army Training & Doctrine Command
ATTN: Tech Library
Fort Monroe, VA 23651

Department of the Air Force
5WW/DN
Langley AFB, VA 23665

Commander
US Army INSCOM/QRC
6845 Elm Street - S407
McLean, VA 22101

MITRE Corporation
ATTN: Robert Finkelstein
1820 Dolley Madison Blvd
McLean, VA 22101

Science Applications, Inc.
8400 Westpark Drive
ATTN: Dr. John E. Cockayne
McLean, VA 22101

Director
Development Center MCDEC
ATTN: Firepower Division
Quantico, VA 22134

US Army Nuclear & Chemical Agency
ATTN: MONA-WE (Dr. Jack Berberet)
7500 Backlick Road
Springfield, VA 22150

Director
US Army Signals Warfare Laboratory
ATTN: DELSW-OS (Dr. R. Burkhardt)
Vint Hill Farms Station
Warrenton, VA 22186

Commander
US Army Cold Regions Test Center
ATTN: STECR-OP-PM
APO Seattle, WA 98733

ATMOSPHERIC SCIENCES RESEARCH PAPERS

1. Lindberg, J.D., "An Improvement to a Method for Measuring the Absorption Coefficient of Atmospheric Dust and other Strongly Absorbing Powders, " ECOM-5565, July 1975.
2. Avara, Elton, P., "Mesoscale Wind Shears Derived from Thermal Winds," ECOM-5566, July 1975.
3. Gomez, Richard B., and Joseph H. Pierluissi, "Incomplete Gamma Function Approximation for King's Strong-Line Transmittance Model," ECOM-5567, July 1975.
4. Blanco, A.J., and B.F. Engebos, "Ballistic Wind Weighting Functions for Tank Projectiles," ECOM-5568, August 1975.
5. Taylor, Fredrick J., Jack Smith, and Thomas H. Pries, "Crosswind Measurements through Pattern Recognition Techniques," ECOM-5569, July 1975.
6. Walters, D.L., "Crosswind Weighting Functions for Direct-Fire Projectiles," ECOM-5570, August 1975.
7. Duncan, Louis D., "An Improved Algorithm for the Iterated Minimal Information Solution for Remote Sounding of Temperature," ECOM-5571, August 1975.
8. Robbiani, Raymond L., "Tactical Field Demonstration of Mobile Weather Radar Set AN/TPS-41 at Fort Rucker, Alabama," ECOM-5572, August 1975.
9. Miers, B., G. Blackman, D. Langer, and N. Lorimier, "Analysis of SMS/GOES Film Data," ECOM-5573, September 1975.
10. Manquero, Carlos, Louis Duncan, and Rufus Bruce, "An Indication from Satellite Measurements of Atmospheric CO2 Variability," ECOM-5574, September 1975.
11. Petracca, Carmine, and James D. Lindberg, "Installation and Operation of an Atmospheric Particulate Collector," ECOM-5575, September 1975.
12. Avara, Elton P., and George Alexander, "Empirical Investigation of Three Iterative Methods for Inverting the Radiative Transfer Equation," ECOM-5576, October 1975.
13. Alexander, George D., "A Digital Data Acquisition Interface for the SMS Direct Readout Ground Station — Concept and Preliminary Design," ECOM-5577, October 1975.
14. Cantor, Israel, "Enhancement of Point Source Thermal Radiation Under Clouds in a Nonattenuating Medium," ECOM-5578, October 1975.
15. Norton, Colburn, and Glenn Hoidale, "The Diurnal Variation of Mixing Height by Month over White Sands Missile Range, N.M," ECOM-5579, November 1975.
16. Avara, Elton P., "On the Spectrum Analysis of Binary Data," ECOM-5580, November 1975.
17. Taylor, Fredrick J., Thomas H. Pries, and Chao-Huan Huang, "Optimal Wind Velocity Estimation," ECOM-5581, December 1975.
18. Avara, Elton P., "Some Effects of Autocorrelated and Cross-Correlated Noise on the Analysis of Variance, " ECOM-5582, December 1975.
19. Gillespie, Patti S., R.L. Armstrong, and Kenneth O. White, "The Spectral Characteristics and Atmospheric CO2 Absorption of the Ho^{+3}:YLF Laser at 2.05μm," ECOM-5583, December 1975.
20. Novlan, David J. "An Empirical Method of Forecasting Thunderstorms for the White Sands Missile Range," ECOM-5584, February 1976.
21. Avara, Elton P., "Randomization Effects in Hypothesis Testing with Autocorrelated Noise," ECOM-5585, February 1976.
22. Watkins, Wendell R., "Improvements in Long Path Absorption Cell Measurement," ECOM-5586, March 1976.
23. Thomas, Joe, George D. Alexander, and Marvin Dubbin, "SATTEL — An Army Dedicated Meteorological Telemetry System," ECOM-5587. March 1976.
24. Kennedy, Bruce W., and Delbert Bynum, "Army User Test Program for the RDT&E-XM-75 Meteorological Rocket," ECOM-5588, April 1976.

25. Barnett, Kenneth M., "A Description of the Artillery Meteorological Comparisons at White Sands Missle Range, October 1974 - December 1974 ('PASS' - Prototype Artillery [Meteorological] Subsystem)," ECOM-5589, April 1976.
26. Miller, Walter B., "Preliminary Analysis of Fall-of-Shot From Project 'PASS'," ECOM-5590, April 1976.
27. Avara, Elton P., "Error Analysis of Minimum Information and Smith's Direct Methods for Inverting the Radiative Transfer Equation," ECOM-5591, April 1976.
28. Yee, Young P., James D. Horn, and George Alexander, "Synoptic Thermal Wind Calculations from Radiosonde Observations Over the Southwestern United States," ECOM-5592, May 1976.
29. Duncan, Louis D., and Mary Ann Seagraves, "Applications of Empirical Corrections to NOAA-4 VTPR Observations," ECOM-5593, May 1976.
30. Miers, Bruce T., and Steve Weaver, "Applications of Meterological Satellite Data to Weather Sensitive Army Operations,"ECOM-5594, May 1976.
31. Sharenow, Moses, "Redesign and Improvement of Balloon ML-566," ECOM-5595, June, 1976.
32. Hansen, Frank V., "The Depth of the Surface Boundary Layer," ECOM-5596, June 1976.
33. Pinnick, R.G., and E.B. Stenmark, "Response Calculations for a Commercial Light-Scattering Aerosol Counter," ECOM-5597, July 1976.
34. Mason, J., and G.B. Hoidale, "Visibility as an Estimator of Infrared Transmittance," ECOM-5598, July 1976.
35. Bruce, Rufus E., Louis D. Duncan, and Joseph H. Pierluissi, "Experimental Study of the Relationship Between Radiosonde Temperatures and Radiometric-Area Temperatures," ECOM-5599, August 1976.
36. Duncan, Louis D., "Stratospheric Wind Shear Computed from Satellite Thermal Sounder Measurements," ECOM-5800, September 1976.
37. Taylor, F., P. Mohan, P. Joseph and T. Pries, "An All Digital Automated Wind Measurement System," ECOM-5801, September 1976.
38. Bruce, Charles, "Development of Spectrophones for CW and Pulsed Radiation Sources," ECOM-5802, September 1976.
39. Duncan, Louis D., and Mary Ann Seagraves,"Another Method for Estimating Clear Column Radiances," ECOM-5803, October 1976.
40. Blanco, Abel J., and Larry E. Taylor, "Artillery Meteorological Analysis of Project Pass," ECOM-5804, October 1976.
41. Miller, Walter, and Bernard Engebos," A Mathematical Structure for Refinement of Sound Ranging Estimates," ECOM-5805, November, 1976.
42. Gillespie, James B., and James D. Lindberg, "A Method to Obtain Diffuse Reflectance Measurements from 1.0 to 3.0 μm Using a Cary 17I Spectrophotometer," ECOM-5806, November 1976.
43. Rubio, Roberto, and Robert O. Olsen,"A Study of the Effects of Temperature Variations on Radio Wave Absorption,"ECOM-5807, November 1976.
44. Ballard, Harold N., "Temperature Measurements in the Stratosphere from Balloon-Borne Instrument Platforms, 1968-1975," ECOM-5808, December 1976.
45. Monahan, H.H., "An Approach to the Short-Range Prediction of Early Morning Radiation Fog," ECOM-5809, January 1977.
46. Engebos, Bernard Francis, "Introduction to Multiple State Multiple Action Decision Theory and Its Relation to Mixing Structures," ECOM-5810, January 1977.
47. Low, Richard D.H.,"Effects of Cloud Particles on Remote Sensing from Space in the 10-Micrometer Infrared Region," ECOM-5811, January 1977.
48. Bonner, Robert S., and R. Newton, "Application of the AN/GVS-5 Laser Rangefinder to Cloud Base Height Measurements," ECOM-5812, February 1977.
49. Rubio, Roberto, "Lidar Detection of Subvisible Reentry Vehicle Erosive Atmospheric Material," ECOM-5813, March 1977.
50. Low, Richard D.H., and J.D. Horn, "Mesoscale Determination of Cloud-Top Height: Problems and Solutions," ECOM-5814, March 1977.

51. Duncan, Louis D., and Mary Ann Seagraves, "Evaluation of the NOAA-4 VTPR Thermal Winds for Nuclear Fallout Predictions," ECOM-5815, March 1977.
52. Randhawa, Jagir S., M. Izquierdo, Carlos McDonald and Zvi Salpeter, "Stratospheric Ozone Density as Measured by a Chemiluminescent Sensor During the Stratcom VI-A Flight," ECOM-5816, April 1977.
53. Rubio, Roberto, and Mike Izquierdo, "Measurements of Net Atmospheric Irradiance in the 0.7- to 2.8-Micrometer Infrared Region," ECOM-5817, May 1977.
54. Ballard, Harold N., Jose M. Serna, and Frank P. Hudson Consultant for Chemical Kinetics, "Calculation of Selected Atmospheric Composition Parameters for the Mid-Latitude, September Stratosphere," ECOM-5818, May 1977.
55. Mitchell, J.D., R.S. Sagar, and R.O. Olsen, "Positive Ions in the Middle Atmosphere During Sunrise Conditions," ECOM-5819, May 1977.
56. White, Kenneth O., Wendell R. Watkins, Stuart A. Schleusener, and Ronald L. Johnson, "Solid-State Laser Wavelength Identification Using a Reference Absorber," ECOM-5820, June 1977.
57. Watkins, Wendell R., and Richard G. Dixon, "Automation of Long-Path Absorption Cell Measurements," ECOM-5821, June 1977.
58. Taylor, S.E., J.M. Davis, and J.B. Mason, "Analysis of Observed Soil Skin Moisture Effects on Reflectance," ECOM-5822, June 1977.
59. Duncan, Louis D. and Mary Ann Seagraves, "Fallout Predictions Computed from Satellite Derived Winds," ECOM-5823. June 1977.
60. Snider, D.E., D.G. Murcray, F.H. Murcray, and W.J. Williams, "Investigation of High-Altitude Enhanced Infrared Backround Emissions" (U), SECRET, ECOM-5824, June 1977.
61. Dubbin, Marvin H. and Dennis Hall, "Synchronous Meteorlogical Satellite Direct Readout Ground System Digital Video Electronics," ECOM-5825, June 1977.
62. Miller, W., and B. Engebos, "A Preliminary Analysis of Two Sound Ranging Algorithms," ECOM-5826, July 1977.
63. Kennedy, Bruce W., and James K. Luers, "Ballistic Sphere Techniques for Measuring Atomspheric Parameters," ECOM-5827, July 1977.
64. Duncan, Louis D., "Zenith Angle Variation of Satellite Thermal Sounder Measurements," ECOM-5828, August 1977.
65. Hansen, Frank V., "The Critical Richardson Number," ECOM-5829, September 1977.
66. Ballard, Harold N., and Frank P. Hudson (Compilers), "Stratospheric Composition Balloon-Borne Experiment," ECOM-5830, October 1977.
67. Barr, William C., and Arnold C. Peterson, "Wind Measuring Accuracy Test of Meteorological Systems," ECOM-5831, November 1977.
68. Ethridge, G.A. and F.V. Hansen, "Atmospheric Diffusion: Similarity Theory and Empirical Derivations for Use in Boundary Layer Diffusion Problems," ECOM-5832, November 1977.
69. Low, Richard D.H., "The Internal Cloud Radiation Field and a Technique for Determining Cloud Blackness," ECOM-5833, December 1977.
70. Watkins, Wendell R., Kenneth O. White, Charles W. Bruce, Donald L. Walters, and James D. Lindberg, "Measurements Required for Prediction of High Energy Laser Transmission," ECOM-5834, December 1977.
71. Rubio, Robert, "Investigation of Abrupt Decreases in Atmospherically Backscattered Laser Energy," ECOM-5835. December 1977.
72. Monahan, H.H. and R.M. Cionco, "An Interpretative Review of Existing Capabilities for Measuring and Forecasting Selected Weather Variables (Emphasizing Remote Means)," ASL-TR-0001, January 1978.
73. Heaps, Melvin G., "The 1979 Solar Eclipse and Validation of D-Region Models," ASL-TR-0002. March 1978.

74. Jennings, S.G., and J.B. Gillespie, "M.I.E. Theory Sensitivity Studies - The Effects of Aerosol Complex Refractive Index and Size Distribution Variations on Extinction and Absorption Coefficients Part II: Analysis of the Computational Results," ASL-TR-0003, March 1978.

75. White, Kenneth O. et al, "Water Vapor Continuum Absorption in the 3.5μm to 4.0μm Region," ASL-TR-0004, March 1978.

76. Olsen, Robert O., and Bruce W. Kennedy, "ABRES Pretest Atmospheric Measurements," ASL-TR-0005, April 1978.

77. Ballard, Harold N., Jose M. Serna, and Frank P. Hudson, "Calculation of Atmospheric Composition in the High Latitude September Stratosphere," ASL-TR-0006, May 1978.

78. Watkins, Wendell R. et al, "Water Vapor Absorption Coefficients at HF Laser Wavelengths," ASL-TR-0007, May 1978.

79. Hansen, Frank V., "The Growth and Prediction of Nocturnal Inversions," ASL-TR-0008, May 1978.

80. Samuel, Christine, Charles Bruce, and Ralph Brewer, "Spectrophone Analysis of Gas Samples Obtained at Field Site," ASL-TR-0009, June 1978.

81. Pinnick, R.G. et al., "Vertical Structure in Atmospheric Fog and Haze and its Effects on IR Extinction," ASL-TR-0010, July 1978.

82. Low, Richard D.H., Louis D. Duncan, and Richard B. Gomez, "The Microphysical Basis of Fog Optical Characterization," ASL-TR-0011, August 1978.

83. Heaps, Melvin G., "The Effect of a Solar Proton Event on the Minor Neutral Constituents of the Summer Polar Mesosphere," ASL-TR-0012, August 1978.

84. Mason, James B., "Light Attenuation in Falling Snow," ASL-TR-0013, August 1978.

85. Blanco, Abel J., "Long-Range Artillery Sound Ranging: "PASS" Meteorological Application," ASL-TR-0014, September 1978.

86. Heaps, M.G., and F.E. Niles, "Modeling the Ion Chemistry of the D-Region: A case Study Based Upon the 1966 Total Solar Eclipse," ASL-TR-0015, September 1978.

87. Jennings, S.G., and R.G. Pinnick, "Effects of Particulate Complex Refractive Index and Particle Size Distribution Variations on Atmospheric Extinction and Absorption for Visible Through Middle-Infrared Wavelengths," ASL-TR-0016, September 1978.

88. Watkins, Wendell R., Kenneth O. White, Lanny R. Bower, and Brian Z. Sojka, " Pressure Dependence of the Water Vapor Continuum Absorption in the 3.5- to 4.0-Micrometer Region," ASL-TR-0017, September 1978.

89. Miller, W.B., and B.F. Engebos, "Behavior of Four Sound Ranging Techniques in an Idealized Physical Enviroment," ASL-TR-0018, September 1978.

90. Gomez, Richard G., "Effectiveness Studies of the CBU-88/B Bomb, Cluster, Smoke Weapon" (U), CONFIDENTIAL ASL-TR-0019, September 1978.

91. Miller, August, Richard C. Shirkey, and Mary Ann Seagraves, "Calculation of Thermal Emission from Aerosols Using the Doubling Technique," ASL-TR-0020, November, 1978.

92. Lindberg, James D. et al., "Measured Effects of Battlefield Dust and Smoke on Visible, Infrared, and Millimeter Wavelengths Propagation: A Preliminary Report on Dusty Infrared Test-I (DIRT-I)," ASL-TR-0021, January 1979.

93. Kennedy, Bruce W., Arthur Kinghorn, and B.R. Hixon, "Engineering Flight Tests of Range Meteorological Sounding System Radiosonde," ASL-TR-0022, February 1979.

94. Rubio, Roberto, and Don Hoock, "Microwave Effective Earth Radius Factor Variability at Wiesbaden and Balboa," ASL-TR-0023, February 1979.

95. Low, Richard D.H., "A Theoretical Investigation of Cloud/Fog Optical Properties and Their Spectral Correlations," ASL-TR-0024, February 1979.

96. Pinnick, R.G., and H.J. Auvermann, "Response Characteristics of Knollenberg Light-Scattering Aerosol Counters," ASL-TR-0025, February 1979.

☆U.S. GOVERNMENT PRINTING OFFICE: 1979 677-017/34